jntes

JOURNAL OF NEW TECHNOLOGIES IN ENVIRONMENTAL SCIENCE

4

2020

No. 4 Vol. 4 ISSN 2544-7017 www.jntes.tu.kielce.pl Kielce University of Technology

CONTENTS

www.jntes.tu.kielce.pl
jntes@tu.kielce.pl

The quarterly printed issues of Journal of New Technologies in Environmental Science are their original versions. The Journal published by the Kielce University of Technology.

ISSN 2544-7017

Doi: 10.53412

Mykola RADCHENKO[1]
Andrii RADCHENKO[1]
Dariusz MIKIELEWICZ[2]
Serhiy FORDUY[1]
Anatolii ZUBAREV[1]
Viktor KHALDOBIN[1]
[1] *Admiral Makarov National University of Shipbuilding, 9 Heroes of Ukraine Avenue, Mykolayiv, Ukraine*
[2] *Gdańsk University of Technology 11/12 Gabriela Narutowicza Street, 80-233 Gdansk, Poland*

Doi: 10.53412/jntes-2020-4.1

A STUDY OF EXHAUST WASTE HEAT RECOVERY IN INTERNAL COMBUSTION ENGINES

Abstract: *The efficiency of exhaust heat recovery in typical integrated energy plant on the base of reciprocating gas engines with absorption lithium-bromide chiller for combined electricity, heat and refrigeration supply of the factory Sandora–PepsiCo Ukraine is analyzed. The reserves of decreasing the heat exhausted into atmosphere are revealed on the base of monitoring data and their realization through conversion into refrigeration for cooling the engine cyclic air is proposed. Some scheme decisions of improved and innovative exhaust heat recovery systems providing deep heat conversing into refrigeration for engine cyclic air cooling are developeded.*

Keywords: *energy plant, trigeneration, exhaust heat recovery, combined electricity, heat and refrigeration*

Introduction

The integrated energy plants (IEP) for combined refrigeration, heat and power supply (trigeneration) have growing application [1, 2]. The reciprocating gas fueled engines are used as prime engines [3, 4]. A widespread application of gas engines in IEP for combined supply of electricity, heat and refrigeration is due to well matching current duties [5, 6]. The gas engines are manufactured as cogeneration engine modules equipped with heat exchangers for producing hot water or steam by using the heat of exhaust gas, intake air and charged gas-air mixture of engines, engine jacket and lubricant oil cooling water [7, 8].

With rise in intake air temperature the efficiency of gas engines and IEP reduces: electricity decreases and specific fuel consumption increases [9, 10]. Therefore, the heat released from the engine and conversed into refrigeration can be used for cooling engine cyclic air [11, 12].

The most widespread absorption lithium-bromide chillers (ACh) of a simple cycle enable to provide cooling air to the temperature of about 15°C with a high coefficient of performance: COP of 0.7 to 0.8 [13, 14]. The most simple in design and cheap are jet devices: thermopressors [15, 16] and ejector chillers (ECh) [17, 18]. The refrigerant ejector chillers (ECh) are able to provide cooling air to the temperature of 10°C and lower but with less COP of 0.2 to 0.35 [19, 20] that requires inlarged heat.

In order to encrease the heat converted into refrigeration the advanced technologies of deep exhaust heat utilization can be used [21, 22] with applying low temperature condensing surfaces [23, 24].

The ECh consist generally of heat exhangers with phase change of refrigerant. So, their efficiency can be improved by intensification of heat transfer in evaporators [25-27] including compact minichannels

[28-30] and condensers [31, 32], by application of advanced coolant (refrigerant) circuits with injector [33] and two-stage cooling by heat conversion in combined chillers [34, 35].

The analysis of the IEP efficiency reveals the presence of large heat losses caused by discrepancy of temperature conditions for efficient performance of ACh and gas engine. So, issuing from the condition of engine maintenance at the appropriate thermal rate that provides its reliable operation, the temperature of a return hot water as a coolant entering the engine cogeneration system from ACh, is limited to design value of 70°C [3-5]. If it is exceeded, a surplus heat of return hot water is rejected to atmosphere.

The excessive heat of return hot water rejected to atmosphere in conventional practice of IEP operation can be converted into refrigeration by ejector chillers.

The purpose of the work is increasing the efficiency of conversing the gas engine exhaust heat into refrigeration to match the performance of absorption chiller and gas engine.

Methodology

The problem of increasing the efficiency of conversing the gas engine recoverable heat into refrigeration is solved for a IEP for combined energy supply of factory Sandora–PepsiCo Ukraine (Nikolaev, Ukraine). The trigeneration plant, equipped with two cogeneration Jenbacher gas engines JMS 420 GS-N.LC (electric power N_e = 1400 kW, heat power N_h = 1500 kW) and a single-stage ACh.

The ACh recovers the heat of engine jacket and lubricant oil cooling water, high temperature charged gas-air mixture and engine exhaust gas to produce a chilled water for technology process cooling and conditioning of air in engine room.

The scheme of the existing system of conversing a gas engine recoverable heat into refrigeration by ACh is presented in Figure 1.

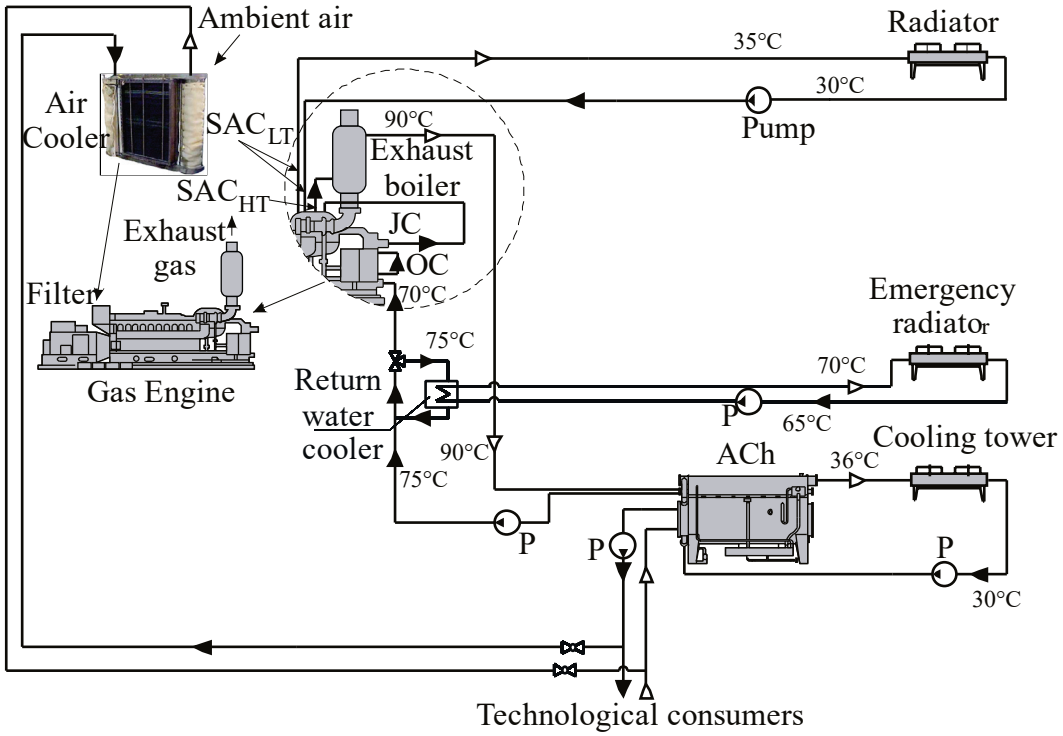

FIGURE 1. *The scheme of the existing system of conversing gas engine recoverable heat into refrigeration by ACh: OC – oil cooler; JC – jacket cooler; SAC_{LT} and SAC_{HT} – low- and high-temperature scavenge air coolers (of charged gas-air mixture)*

According to the conventional scheme in Figure 1 the temperature of return hot water from ACh t_r is about 75°C to 80°C, i.e. above its design value of $t_{r.sp}$ = 70°C at the inlet of heat exchangers of

cogeneration engine module, providing appropriate engine thermal rate. Therefore, a part of return water is cooled in a return water cooler (RWC) with rejecting excessive heat by emergency radiator into the atmosphere.

Return of excessive heat to a single-stage absorption chiller is impossible because of its temperature t_r = 75°C, ..., 80°C lowered than design temperature of the supply hot water for a single-stage absorption chiller: $t_{h.sp}$ = 90°C, ..., 95°C. Fall of the supply hot water temperature would cause dropping the efficiency of transforming a gas engine recoverable heat into a refrigeration in a single-stage absorption chiller – decrease in coefficient of performance (COP) from nominal (design) value of about 0.7 to 0.5 and lower.

In order to estimate a magnitude of excessive heat rejected to the atmosphere and to reveal the reserves for its reduction through returning the heat exhausted to the exhaust heat recovery cycle to produce the additional refrigeration, the analyses of the data on hot water temperatures t_w, received during monitoring of IEP parameters, have been made.

The temperatures of supply hot water t_{w1} to ACh from cogeneration engine module, of return hot water after ACh t_{w4} (before return water cooler RWC for rejecting excess heat by emergency radiator to the atmosphere) and of return hot water, cooled by rejecting excessive heat to the atmosphere (after RWC), i.e. hot coolant at the inlet of gas engine module t_{w5} are given in Figure 2.

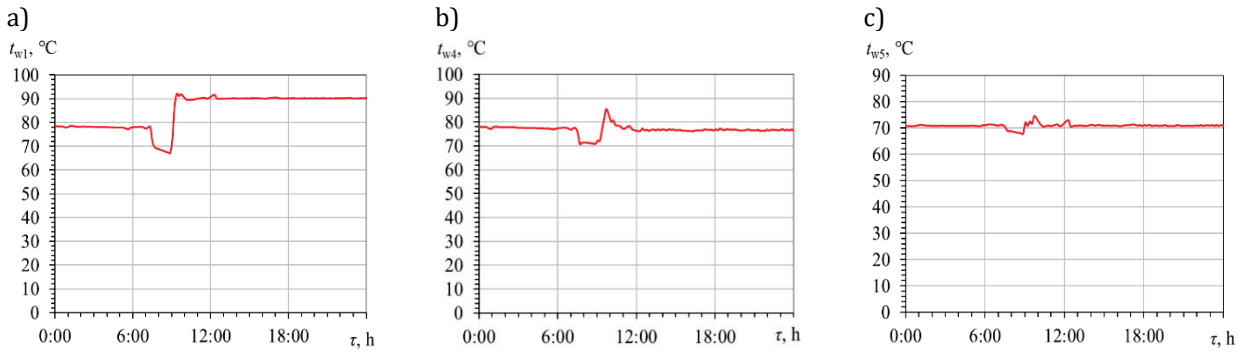

FIGURE 2. *Temperatures of supply hot water t_{w1} to ACh (a); return hot water after ACh t_{w4} (b) and cooled return hot water at the inlet of gas engine t_{w5} (c)*

Temperature difference of supply hot water to ACh and return hot water after it, i.e. temperature drop of hot water in the ACh, $t_{w1} - t_{w4}$, and temperature difference of return hot water from ACh and cooled return hot water at the inlet of gas engine, i.e. temperature drop of return hot water due to rejecting excessive heat to the atmosphere, $t_{w4} - t_{w5}$, are given in Figure 3.

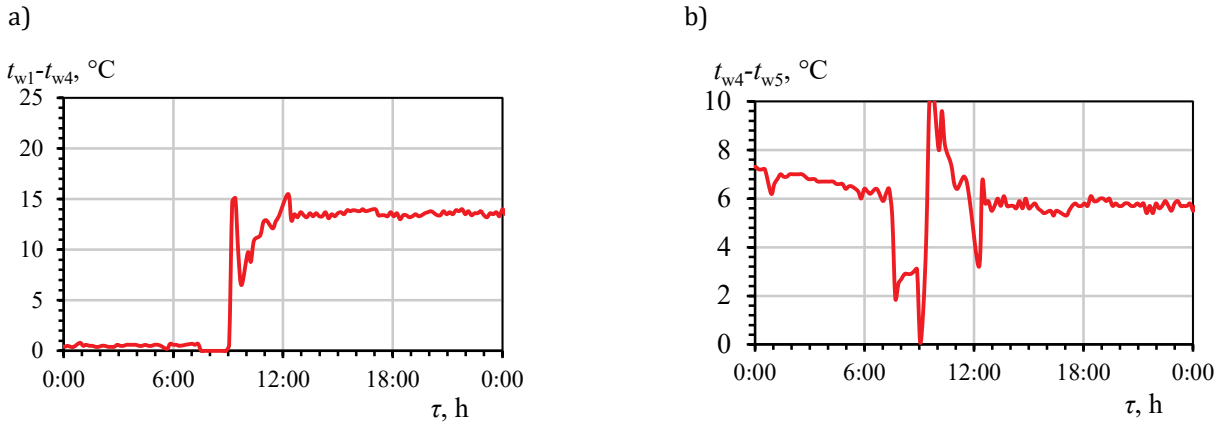

FIGURE 3. *Temperature drops of hot water in ACh $t_{w1} - t_{w4}$ (a) and of return hot water due to rejecting excessive heat to the atmosphere $t_{w4} - t_{w5}$ (b)*

As Figure 3 shows, that temperature drops of hot water in the absorption chiller, $t_{w1} - t_{w4}$, are closed to their design value of 15°C. Meanwhile, the temperature drops of return hot water caused by rejecting excess heat to the atmosphere are rather essential: $t_{w4} - t_{w5} \approx 5$°C, that testifies to considerable heat wasted.

Results

The results of calculations of the heat Q_w rejected to the atmosphere were compared with heat Q_{hA} used by ACh (Fig. 4).

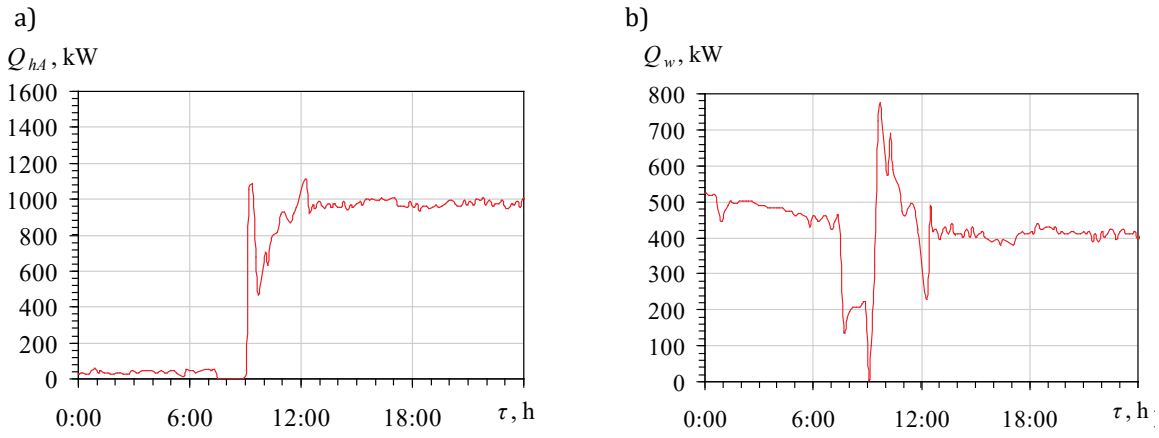

FIGURE 4. *Valueses of heat used by absorption chiller Q_{hA} (a) and heat rejected to the atmosphere Q_w (b)*

The share of heat rejected to the atmosphere Q_w caused by necessity to maintain the temperature of cooled return hot water (hot coolant for gas engine) at the input of gas engine module at the rate of 70°C, is about 40% of heat consumed by ACh and actually third of cogeneration engine module thermal capacity 1400 kW.

The heat recovery system with using the excessive heat (normally rejected to the atmosphere) in ejector chiller (ECh) to produce addition cold for gas engine cyclic air cooling was developed and its efficiency was estimated based on the monitoring data.

It is possible to avoid heat losses inherent in the typical heat recovery system by increasing a temperature rate of excessive heat (normally rejected to the atmosphere) up to design value of 90°C, …, 95°C to be used as activation heat source for ACh. A gas boiler, normally available at any factory as booster boiler, can be applied to heat up the return hot water. So, an additional return hot water circulating contour with booster gas boiler might be integrated into the existing heat recovery system (Fig. 5).

Actual refrigeration capacities of ACh using the currently available heat excluding heat losses caused by rejecting excessive heat to the atmosphere (without heating up the return hot water) Q_{0A} and additional refrigeration capacities Q_{0w} due to recovering excessive heat boosted by gas boiler Q_w are given in Figure 6.

As one can see, due to recovering excessive heat Q_w, normally rejected to the atmosphere, it is possible to maximize the recovery of the available thermal energy and to increase refrigeration capacity of the actual trigeneration plant by Q_{0w} = 300 kW, picking it by about 50% up to design refrigeration capacity of a trigeneration Jenbacher gas engine module JMS 420 GS-N.LC: $Q_{0A} + Q_{0w}$ = 1000 kW.

First of all it should be noted, that the approach to transform the gas engine exhaust heat into refrigeration by ACh of a simple cycle through increasing a temperature rate of excessive heat of

return hot water (excessive heat normally rejected to the atmosphere) up to desirable value (Fig. 5) is the most efficient for multi engines IEP with at least two ACh. In this case the addition heat is used for boosting the heat feeding to the second ACh thereby increasing the refrigeration capacity and the flexibility of the trigeneration plant operation in the whole. The increased refrigeration capacity can be used for gas engine cyclic air cooling to enlarge the engine power output and electricity production as a result, accompanied by reduction of specific fuel consumption.

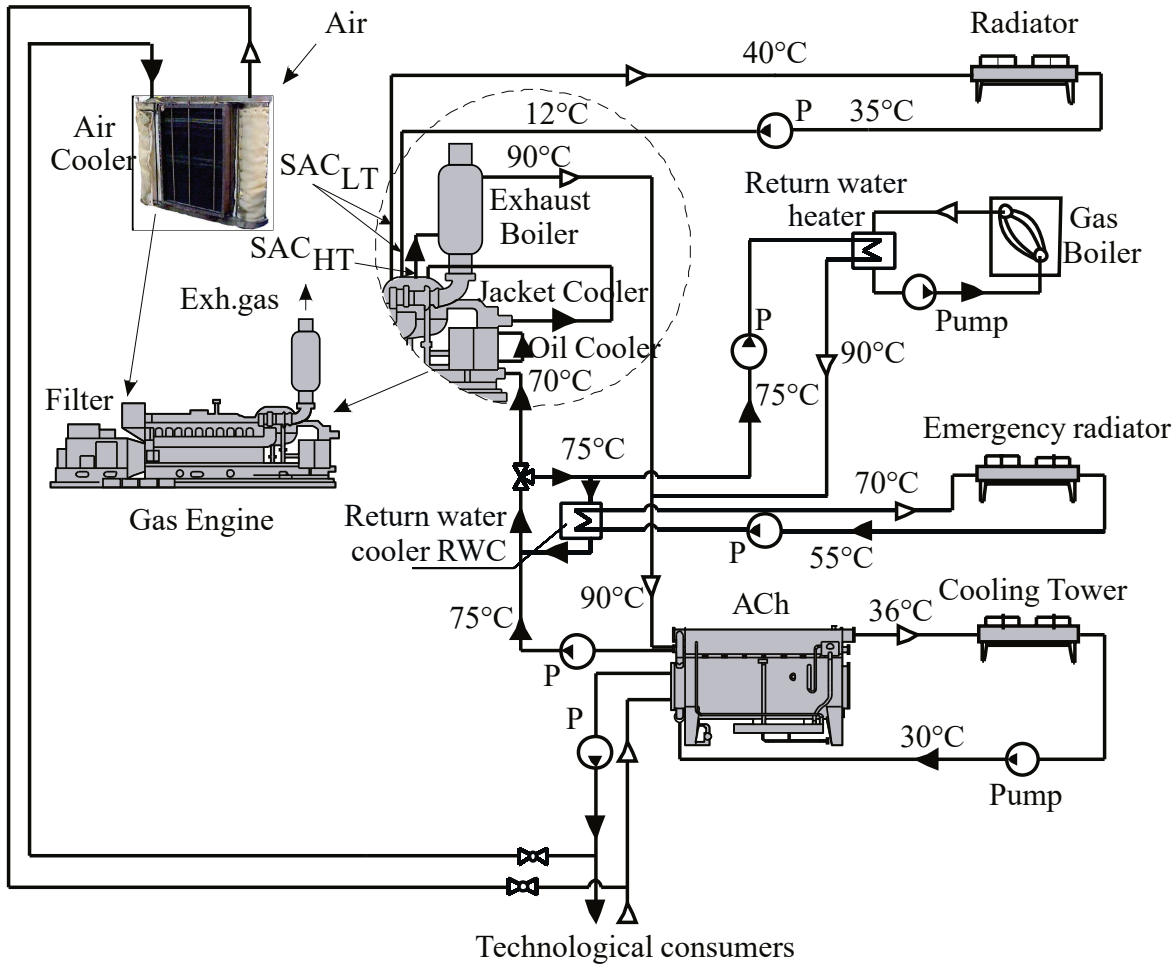

FIGURE 5. *The scheme of modified system of transforming gas engine recoverable heat into refrigeration by absorption chiller: SAC_{LT} and SAC_{HT} – low- and high-temperature scavenge air coolers of charged gas-air mixture*

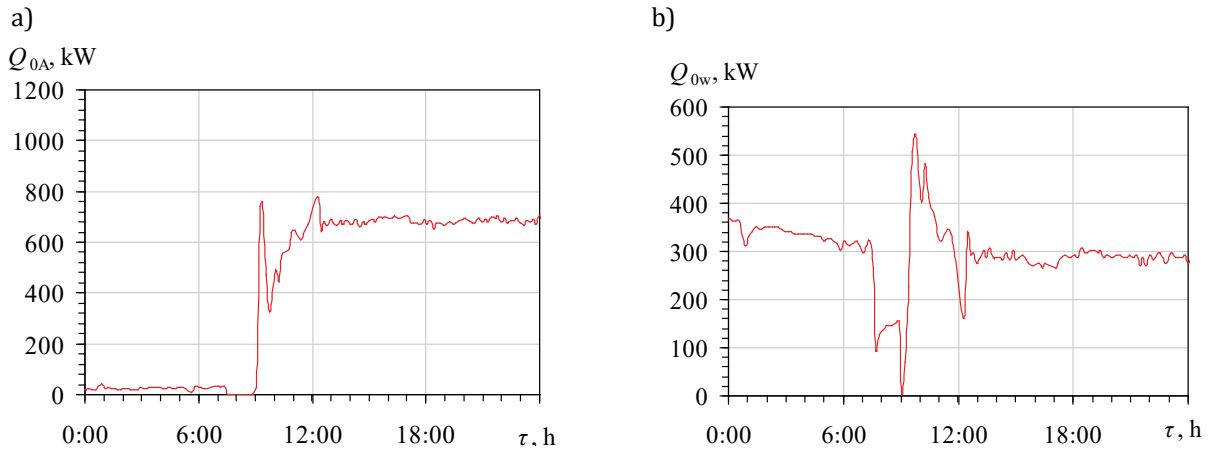

FIGURE 6. *Refrigeration capacities of ACh without boosting excessive heat Q_{0A} (a) and additional refrigeration capacities Q_{0w} due to recovering excessive heat Q_w (b)*

The simplest in implementation and most expedient solution to recover the relatively low-temperature heat of return hot water from ACh of the rate of 75°C, …, 80°C is the application of ejector chiller (ECh) as a low temperature stage of two-stage absorption-ejector chiller (AECh) with ACh as a high temperature stage [34, 35].

The additional refrigeration capacity, gained due to deep recovering the heat exhausted from the engine, is used for engine cyclic air cooling: intake air at the suction of turbocharger in two-stage air cooler with boiling refrigerant of ECh in the low temperature stage and chilled water from ACh in the high temperature stage of air cooler and scavenge air-gas mixture cooling through using chilled water from ACh for subcooling the scavenge air cooling water, precooled in radiator by ambient air, in booster cooler after radiator (Fig. 7).

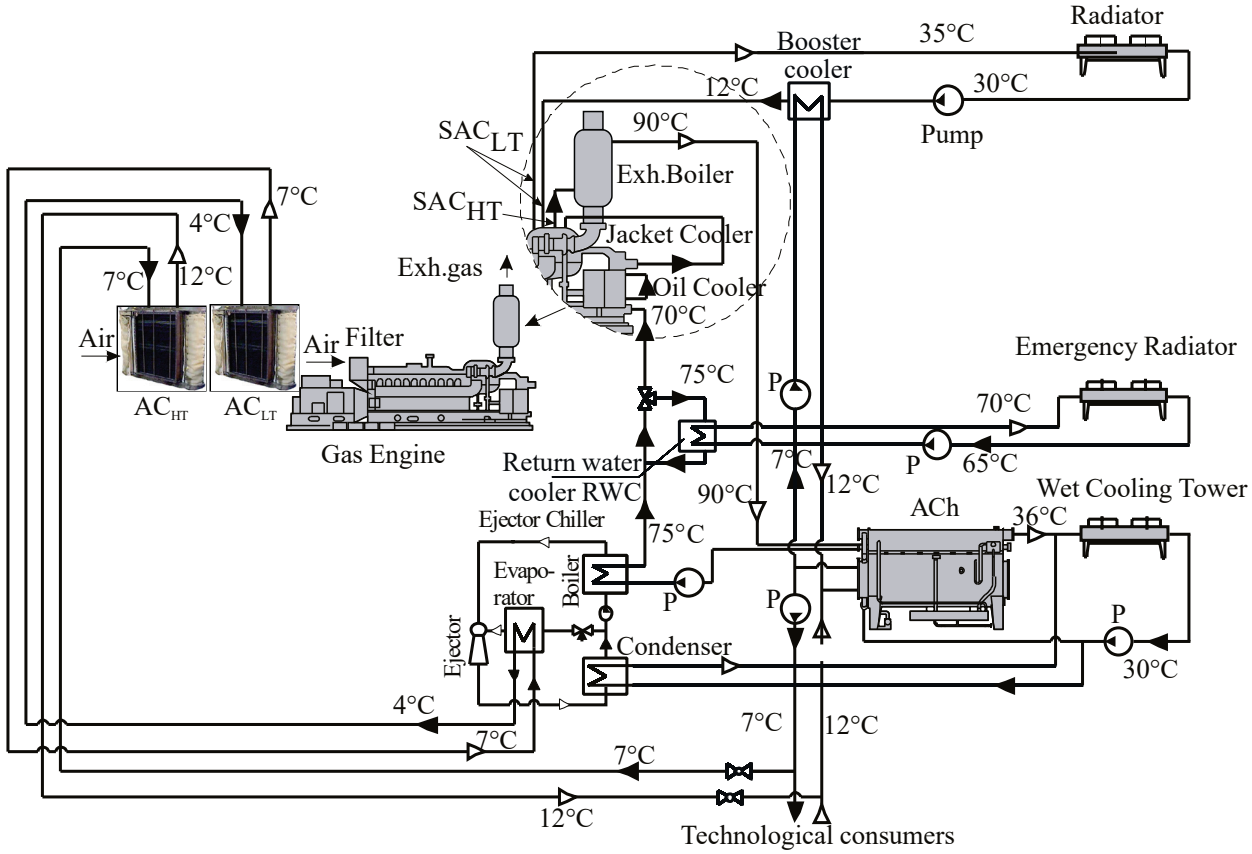

FIGURE 7. *The scheme of innovative system of deep transforming the gas engine exhaust heat by combined AECh: SAC_{LT} and SAC_{HT} – low- and high-temperature scavenge air coolers of charged gas-air mixture; AC_{LT} and AC_{HT} – low- and high-temperature air coolers of engine intake air*

Such engine in-cycle trigeneration provides enhancing engine fuel efficiency and prolong the time of efficient operation of trigeneration plant since cooling demands for technological needs have, as a rule, periodic character.

Conclusions

The analysis of conversing the exhaust heat from gas engine of IEP into refrigeration by ACh, based on monitoring data, has revealed the considerable heat losses of about 40% of ACh heat consumption and actually third of cogeneration engine module thermal capacity 1400 kW, caused by conflicting requirements of temperature conditions for effective performance of ACh and gas engine. So, issuing from the condition of engine maintenance at the appropriate thermal rate that provides its reliable operation, the temperature of a return hot water (as hot coolant for gas engine) entering the engine cogeneration system from ACh, is limited to the value of 70°C. If it is exceeded, a surplus heat of return hot water is rejected to atmosphere.

The approach to transform the gas engine exhaust heat into refrigeration by ACh of a simple cycle through increasing a temperature rate of excessive heat of return hot water (excessive heat normally rejected to the atmosphere) up to desirable value is discussed as the most efficient for multi engines IEP with at least two ACh. With this the addition heat is used for boosting the heat feeding to the second ACh thereby increasing the refrigeration capacity and the flexibility of the trigeneration plant operation in the whole.

The innovative heat recovery system with using the excessive heat (normally rejected to the atmosphere) in ejector chiller (ECh) to produce addition refrigeration capacity for gas engine cyclic air cooling was proposed as the simplest regarding to the implementation and the most expedient solution to recover the relatively low-temperature heat of return hot water from ACh of the rate within 75°C to 80°C.

Two-stage absorption-ejector chiller (AECh) with ejector chiller (ECh) as a low temperature stage and ACh as a high temperature stage is proposed to utilize the advantages of each chiller.

Two-stage gas engine inake air cooling system with boiling refrigerant of ECh in the low temperature stage and chilled water from ACh in the high temperature stage of air cooler.

Therefore it is reasonable to apply ECh as a low temperature stage and ACh as a high temperature stage of two-stage absorption-ejector chiller (AECh). A combined AECh is able to provide engine cyclic air deep cooling and enhance engine fuel efficiency.

Such in-cycle trigeneration provides engine cyclic air deep cooling leads to enhancing engine fuel efficiency and prolonging the time of efficient operation of trigeneration plant, since cooling demands for technological needs have, as a rule, periodic character.

Conflicts of Interest: The author declares no conflict of interest.

References

[1] Canova A., Cavallero C., Freschi F., Giaccone L., Repetto M., Tartaglia M., *Optimal energy management*, IEEE Industry Applications Magazine, Vol. 15, 2009, pp. 62-65.

[2] Ortiga J., Bruno J.C., Coronas A., *Operational optimization of a complex trigeneration system connected to a* district *heating and cooling network*, Applied Thermal Engineering, Vol. 50, 2013, pp. 1536-1542.

[3] *Cogeneration & Trigeneration – How to produce energy efficiently. A practical guide for experts in emerging and developing economies*, Zellner S., Burgtorf J., Kraft-Schäfer D. (eds.), Deutsche Gesellschaft für Internationale Zusammenarbeit (GIZ) GmbH, 2016, p. 144.

[4] Gluesenkamp K., Hwang Y., Radermacher R., *High efficiency micro trigeneration systems*, Applied Thermal Engineering, Vol. 50, 2013, p. 6.

[5] *CIMAC position paper gas engine aftertreatment systems by CIMAC WG 17*, Gas Engines, May 2017, https://www.cimac.com/cms/upload/Publication_Press/WG_Publications/CIMAC_WG17_2017_Aug_Position_Paper_Gas_Engine_Aftertreatment_Systems.pdf.

[6] *Jenbacher*, http://www.intma.ru/energetica/power_stations/thermal_ps_trigeneration_ru.html.

[7] Rouse G., Czachorski M., Bishop P., Patel J., *GTI Integrated Energy System for Buildings. Modular System Prototype*, GTI Project report 15357/65118: Gas Technology Institute (GTI), January 2006, p. 495.

[8] Elsenbruch T., *Jenbacher gas engines a variety of efficient applications*, Bucureşti, 28 October 2010, p. 73.

[9] Radchenko A., Mikielewicz D., Forduy S., Radchenko M., Zubarev A., *Monitoring the fuel efficiency of gas engine in integrated energy system* [in:] Nechyporuk M. et al. (eds.), ICTM 2019, AISC, Springer, Vol. 1113, Cham 2020, pp. 361-370.

[10] Forduy S., Radchenko A., Kuczynski W., Zubarev A., Konovalov D., *Enhancing the fuel efficiency of gas engines in integrated energy system by chilling cyclic air* [in:] Tonkonogyi V. et al. (eds.), Grabchenko's ICAMP, InterPartner-2019, LNME, Springer, Cham 2020, pp. 500-509.

[11] Trushliakov E., Radchenko A., Forduy S., Zubarev A., Hrych A., *Increasing the operation efficiency of air conditioning system for integrated power plant on the base of its monitoring* [in:] Nechyporuk M. et al. (eds.), (ICTM 2019), AISC (2020), Springer, Vol. 1113, Cham 2020, pp. 351-360.

[12] Radchenko A., Scurtu I.-C., Radchenko M., Forduy S., Zubarev A., *Monitoring the efficiency of cooling air at the inlet of gas engine in integrated energy system*, Thermal Science 2020 OnLine-First Issue 00, pp. 344-344, https://doi.org/10.2298/TSCI200711344R.

[13] Radchenko A., Stachel A., Forduy S., Portnoi B., Rizun O., *Analysis of the efficiency of engine inlet air chilling unit with cooling towers* [in:] Ivanov V. et al. (eds.), ADSM III (DSMIE 2020), LNME, Springer, Cham 2020, pp. 322-331.

[14] Radchenko M., Portnoi B., Kantor S., Forduy S., Konovalov D., *Rational thermal loading the engine inlet air chilling complex with cooling towers* [in:] Tonkonogyi V. et al. (eds.), AMP II, InterPartner 2020, LNME, Springer, Cham 2021, pp. 724-733.

[15] Konovalov D., Kobalava H., Radchenko M., Scurtu I.C., Radchenko R., *Determination of hydraulic resistance of the aerothermopressor for gas turbine cyclic air cooling* [in:] TE-RE-RD 2020, E3S Web of Conferences, Vol. 180, 2020, No. 01012.

[16] Konovalov D., Trushliakov E., Radchenko M., Kobalava G., Maksymov V., *Research of the aerothermopresor cooling system of charge air of a marine internal combustion engine under variable climatic conditions of operation* [in:] Tonkonogyi V. et al. (eds.), ICAMP, InterPartner-2019, LNME, Springer, Cham 2020, pp. 520-529.

[17] Radchenko R., Kornienko V., Pyrysunko M., Bogdanov M., Andreev A., *Enhancing the efficiency of marine diesel engine by deep waste heat recovery on the base of its simulation along the route line* [in:] Nechyporuk M. et al. (eds.), ICTME, AISC, Springer, Vol. 1113, Cham 2020, pp. 337-350.

[18] Radchenko R., Pyrysunko M., Radchenko A., Andreev A., Kornienko V., *Ship engine intake air cooling by ejector chiller using recirculation gas heat* [in:] Tonkonogyi V. et al. (eds.), AMP, InterPartner-2020, LNME, Springer, Cham 2021, pp. 734-743.

[19] Butrymowicz D., Gagan J., Śmierciew K., Łukaszuk M., Dudar A., Pawluczuk A., Łapiński A., Kuryłowic A., *Investigations of prototype ejection refrigeration system driven by low grade heat*, HTRSE-2018, E3S Web of Conferences 2018, Vol. 70, p. 7.

[20] Smierciew K., Gagan J., Butrymowicz D., Karwacki J., *Experimental investigations of solar driven ejector air-conditioning system*, Energy and Buildings, Vol. 80, 2014, pp. 260-267.

[21] Kornienko V., Radchenko M., Radchenko R., Konovalov D., Andreev A., Pyrysunko M., *Improving the efficiency of heat recovery circuits of cogeneration plants with combustion of water-fuel emulsions*, Thermal Science, Vol. 25, Issue 1, Part B, 2021, pp. 791-800.

[22] Kornienko V., Radchenko R., Konovalov D., Andreev A., Pyrysunko M., *Characteristics of the rotary cup atomizer used as afterburning Installation in exhaust gas boiler flue* [in:] Ivanov V. et al. (eds.), ADSM III(DSMIE 2020), LNME, Springer, Cham 2020, pp. 302-311.

[23] Kornienko V., Radchenko R., Stachel A., Andreev A., Pyrysunko M., *Correlations for pollution on condensing surfaces of exhaust gas boilers with water-fuel emulsion combustion* [in:] Tonkonogyi V. et al. (eds.), AMP, InterPartner-2019, LNME, Springer, Cham 2020, pp. 530-539.

[24] Kornienko V., Radchenko R., Bohdal Ł., Kukiełka L., Legutko S., *Investigation of condensing heating surfaces with reduced corrosion of boilers with water-fuel emulsion combustion* [in:] Nechyporuk M. et al. (eds.), ICTM 2020, LNNS, Springer, Vol. 188, Cham 2021, pp. 300-309.

[25] Dąbrowski P., Klugmann M., Mikielewicz D., *Selected studies of flow maldistribution in a minichannel plate heat exchanger*, Archives of Thermodynamics, Vol. 38, 2017, pp. 135-148.

[26] Kumar R., Singh G., Mikielewicz D., *A new approach for the mitigating of Flow Maldistribution in Parallel Microchannel Heat Sink*, Journal of Heat Transfer, Vol. 140, 2018, pp. 72401-72410.

[27] Kumar R., Singh G., Mikielewicz D., *Numerical study on mitigation of flow maldistribution in parallel microchannel heat sink: channels variable width versus variable height approach*, Journal of Electronic Packaging, Vol. 141, 2019, pp. 21009-21011.

[28] Dąbrowski P., Klugmann M., Mikielewicz D., *Channel blockage and flow maldistribution during unsteady flow in a model microchannel plate heat exchanger*, Journal of Applied Fluid Mechanics, Vol. 12, 2019, pp. 1023-1035.

[29] Mikielewicz D., Klugmann M., Wajs J., *Flow boiling intensification in minichannels by means of mechanical flow turbulising inserts*, International Journal of Thermal Sciences, Vol. 65, 2013, pp. 79-91.

[30] Bohdal T., Kuczynski W., *Boiling of R404A refrigeration medium under the conditions of periodically generated disturbances*, Heat Transf. Eng., Vol. 32, 2011, pp. 359-368, doi:10.1080/01457632.2010.483851.

[31] Kuczyński W., Charun H., *Experimental investigations into the impact of the void fraction on the condensation characteristics of R134a refrigerant in minichannels under conditions of periodic instability*, Arch. Thermodyn., Vol. 32, 2011, pp. 21-37, doi:10.2478/v10173.

[32] Kuczyski W., Charun H., Bohdal T., Kuczynski W., *Influence of hydrodynamic instability on the heat transfer coefficient during condensation of R134a and R404A refrigerants in pipe minichannels*, Int. J. Heat Mass Transf., Vol. 55, 2012, pp. 1083-1094, doi:10.1016/j.ijheatmasstransfer.2011.10.002.

[33] Trushliakov E., Radchenko M., Bohdal T., Radchenko R., Kantor S., *An innovative air conditioning system for changeable heat loads* [in:] Tonkonogyi V. et al. (eds.), ICAMP, InterPartner-2019, LNME, Springer, Cham 2020, pp. 616-625.

[34] Radchenko A., Trushliakov E., Kosowski K., Mikielewicz D., Radchenko M., *Innovative turbine intake air cooling systems and their rational designing*, Energies, 2020, Vol. 13, Issue 23, No. 6201.

[35] Radchenko R., Radchenko N., Tsoy A., Forduy S., Zybarev A., Kalinichenko I., *Utilizing the heat of gas module by an absorption lithium-bromide chiller with an ejector booster stage*, AIP Conference Proceedings, Vol. 2285, 2020, No. 030084.

Maciej KOTUŁA[1, 3]
Aleksander SZKAROWSKI[1, 2]
Aleksandr CHERNYKH[2]
[1] *Koszalin University of Technology, Poland*
[2] *St. Petersburg State University of Architecture & Civil Engineering, Russia*
[3] Corresponding authors e-mail: maciej-kotula@wp.pl

Doi: 10.53412/jntes-2020-4.2

RESEARCH OF WATER CONDENSATION IN GAS TRANSMISSION PIPELINES

Abstract: *The domestic gas industry has been set an ambitious goal in the form of a state programme for extensive gasification of Polish cities and towns. This provides for transition of the municipal thermal energy and of the municipal economy to natural gas. Ensuring of reliable and safe transport of the gaseous fuel is also a part of this programme. The article discusses the problems of transporting of the nitrogen-rich natural gas from the local mines, related to water of unknown origin appearing in it. The events that can confirm that there is a possibility of moisture condensation from the gas and its migration deep into the distribution network have been analysed. The actual level of moisture in the natural gas, which is already directly supplied to the consumers, has been experimentally tested. It has been proved by the computer calculations that in the conditions of high pressure in the network, there is a possibility of such condensation, depending on the external atmospheric conditions and physicochemical parameters of the gas. It has been proposed to change the existing designing and construction legal provisions in order to protect the gas networks against water accumulating in them in a better way.*

Keywords: *natural gas, water condensation, gas transport, high pressure, gas moisture.*

Introduction

The historical orientation of the fuel balance of Poland towards solid fuel causes huge technical, economic and ecological problems for the country, also on an international scale. The Polish government has announced a broad programme of ensuring of energy security of the country by diversification of the natural gas supply from various sources and directions thanks to the effective use of the LNG terminal on the Polish coast and creation of new cross-border connections (Project 2019). It anticipates development of the gas supply industry in the coming years and at an unprecedented pace [6].

Therefore, technologically advanced, effective and environmentally friendly conversion of the domestic heat power engineering and municipal economy into gas fuel becomes a call for the Polish gas industry. It is these devices that constitute the most numerous and very dispersed group of thermal technology devices. Currently, they are characterised by low efficiency and significant impact on environmental pollution in the places where people live and work. The exhaust fumes from these devices are discharged into the atmosphere through low chimneys or just above the roof of buildings. The issue of the global warming and the obligations of Poland to reduce greenhouse gas emissions are also significant. Combustion of natural gas ensures CO_2 emissions that are almost twice lower compared to hard coal (the maximum content of carbon dioxide in natural gas flue gas is 11.8% by volume in comparison with 21% by volume for coal).

In the conditions of the anticipated development of the domestic gas industry, the key issue is to increase the capacity of the Polish natural gas transmission network and to ensure reliability of the gas

supply process as well as its appropriate quality [5]. One of the acute problems from this point of view is the moisture content of the gas fuel [9]. This problem is further intensified by the increasing scale of the use of the liquefied natural gas being technologically associated with the cryogenic processes.

Analysis of the principles for gas supply in terms of moisture content

It is not widely known that water may appear in the gas pipelines that distribute the natural gas directly to the consumers. On the other hand, the specialists in the field of operation of the gas networks deal with this phenomenon on a daily basis. Where does this water come from? Certainly not through the leakage places arising on the network due to mechanical damage or corrosion, as the gas pipeline is always under positive pressure.

The natural gas extracted from the ground is usually contaminated with solid fractions and loaded with moisture as well as has caustic properties. The previously dried gas taken from the underground gas storage facilities is also saturated with water. The presence of water in the natural gas is undesirable because it intensifies corrosion of pipes and equipment, especially in the presence of H_2S and CO_2, while in winter it forms ice plugs. It may also contribute to formation of the hydrates that block the flow of the gas, especially in case of liquid hydrocarbon recovery processes, such as freezing or cryogenic processes [1].

Moisture removal is the key stage in the pre-treatment of the natural gas directly at the point of its extraction and further processing before sale. Over the time, a stereotype that "dry gas" should be delivered to the consumers has developed. In the aforementioned PN-C-04753 standard, humidity of the gas is not even mentioned among "the values relevant for the assessment of gas quality". This stereotype resulted in the fact that the dehydrators installed previously at each connection and even under the gas installation risers disappeared from the designing practice.

In fact, the dried natural gas cannot be "dry", i.e. completely devoid of moisture. Even the already criticised standard, not setting any requirements in the field of the moisture content in the gas, paradoxically speaks about the processes that "may cause formation of water condensates". The resulting contradiction is also based on the measurement technology. Using the chromatographic analysis methods to determine the gas fuel composition, the sample is first subjected to drying. Therefore, the analysis shows not moist ("real" or "working"), but so-called "dry" gas composition, without the moisture content.

The gas suppliers are aware of the contradiction described above. To ensure adequate gas properties, the transmission network operators provide declarations regarding the properties of the transmitted fuel on their official sites. They include *inter alia* the permissible moisture content in the form of the maximum dew point temperature t_r, separately for summer and winter. The safety of the gas in transport and further use depends on it directly and its efficiency is important from the point of view of fulfilment of the contractual tax obligations [3].

The t_r value in the certificates analysed in the work [9] ranged from +4°C to –6°C. In general, these values are very close to the requirements for the gas quality in the transmission networks [4] (–5°C in winter and up to +3.7°C in summer). However, tests of the gas samples taken from the network showed that the dew point temperature could reach even +20°C. This means that in the winter season gas saturation with water vapour with its subsequent condensation is inevitable. It may be therefore concluded that determination of the t_r value, which may possibly be higher than the gas distribution temperature, in the certificate indicates a high probability of condensation forming in the gas pipelines.

The dew point means that water in the gas composition is in a saturated state, i.e. the partial pressure of the water vapour p_p is equal to the water saturation pressure p_p^n at a given temperature. For example, at 0°C $p_p = p_p^n = 611$ Pa [8]. The thermodynamic calculations show that under normal conditions (0°C and 101325 Pa) the absolute humidity of the gas in the saturated state (water vapour

content in 1 m^3 of the moist gas) is 4.88 g/m^3 and the molar share of the water vapour corresponding to the dew point is 0.0061 (0.61% by volume).

The financial conclusions are quite obvious. If gas humidity only oscillates on the edge of the dew point, an example boiler room that needs 1 million m^3 of the gas annually "consumes" over 6000 m^3 of the water vapour in its composition. The meter indicates this volume as the gas and the user pays for it. In addition, 1% of the water vapour by volume reduces the calorific value of E-group high-methane gas by approx. 0.37 MJ/m^3, which is more than 1% [9]. The efficiency of the gas devices is proportionally reduced.

However, the hazards arising during the operation of the gas networks in case of presence of the condensed water in the gas pipelines are much more important. That is why it is so important to analyse each failure and the resulting conclusions thoroughly – in terms of the causes of the abnormal states and disturbance of the stability of the supervised systems as well as of the ways to prevent such events in the future. The authors have attempted to conduct such analysis on the basis of the gathered data on gas network failures and their own measurements.

Analysis of failure causes connected with natural gas waterlogging

The analysed failures have different scale, reach and publicity in the media. The most well-known failures include the one of the Russian gas transit system (supplier – Russian State Concern Gazprom), when the Polish customer (Operator Gazociągów Przesyłowych Gaz-System S.A.) announced suspension of all gas supplies from the Yamal gas pipeline on 22 June 2017. This was done due to the failure of the Russian gas drying instance in fear of the safety of the Polish gas pipelines. In this information, it was stated that Poland did not have its own installation for drying of such gas flows and that the closest one was in Germany.

Despite the international scale of the failure and huge quantities of the raw material, it did not affect the gas supplies for the consumers. The gas tanks performed their task and already on 23 June 2017 at 6:00 a.m., due to improvement of the quality parameters of the natural gas, Gaz-System resumed reception of the fuel to the national transmission system at the Interconnection Point. Therefore, it can be considered an accidental phenomenon, as in general, the gas drying installations at Gazprom operate in a faultless way. The most commonly used solutions are glycol installations and the supply system is stabilised in such a way that it provides the opportunity to choose the optimal time of contact of the gas with the glycols. Even the effective trade agreements ensure such stabilisation of supplies, as in case of lower consumption, the generated surplus of the transit gas is injected into the underground warehouses all over Europe.

The gas drying cycles operate in a much worse way in the regional gas distribution systems based mainly on the local wells with the nitrogen-rich gas mines. These systems are characterised by large fluctuations of the flows during the transitional periods (spring and autumn), in case of sudden changes of the weather and even during the day. Then, the drying processes encounter a big problem due to lack of the possibility to stabilise the gas-glycol contact time. This situation occurs in all distribution networks in Poland supplying the L_w and L_s subgroup natural gas to the customers.

The entire coastal zone in the central part of western Pomerania, including Kołobrzeg, is supplied with the natural gas from the L_s subgroup. In the distribution systems, there are still some engineering interventions aimed at ensuring of high quality of the gas supply as well as of widely-understood security. Such events are both planned and unexpected, classified as failures. They are thoroughly analysed in terms of potential threats and undesirable effects. A number of instructions, guidelines and regulations, which together form a specific technological regime in the field of designing, construction and operation of each distribution network, are created.

Many typical failures are currently very well analysed and described in the field of the actions to be taken. Even the failures that are very well known to the public are often typical and the extent of their

consequences determines their publicity. Another type of the events includes the ones which surprise the specialists, since they do not have well-developed and proven methods of action.

One of such unexplained failures on the low-pressure gas network was the sudden suspension of the natural gas supply to the Spa District in Kołobrzeg in February 2016. Kołobrzeg has a specific layout. The Spa District, situated along the coastline, is practically "cut off" from the rest of the city by railway tracks. This results in difficult access to it in terms of the road, municipal as well as gas infrastructure. Development of the heating technology based on the natural gas has quickly forced an increase of the gas supply to this district.

At that time, at the end of the 1980s, the technology of construction of the polyethylene pipe networks was not used in Poland yet and the gas was supplied to the customers only by low-pressure networks (1.3-1.6 kPa). It was a natural solution to replace the supply gas pipeline with 100-150 mm diameter with a new one with 300 mm diameter. For many subsequent years, the gas was supplied to the district in a stable manner and the occurring slight pressure drops were explained by the continuous increase of the demand resulting from expansion of the existing facilities and construction of the new ones. Over the time, more and more pressure problems began to appear, especially in winter during the holidays. On 2 February 2016, the employees of the Gasworks in Kołobrzeg recorded numerous reports on lack of gas pressure.

Pressure measurements at the sampling points showed unacceptable values in the range of 0.65-0.82 kPa. At that time, the reduction stations supplied the gas at the right pressure with a large capacity reserve. This indicated that the main gas pipeline was no longer permeable. The network layout and the foundation ordinates, the pressure measurements, the lay as well as the type of land development and utilities were analysed. As a result of this analysis, the characteristic points on the gas network where the control excavations had to be made were selected. Measurements were made with the use of a double bag-positioning device. In this way, the search site narrowed to a section of about 15.0 m at the lowest point of the terrain.

After cutting of the pipe, water escaped from it instead of the gas and a pump was installed instead of the bag-positioning device. In total, about 500 litres of water were pumped out, which meant geometrically that a section of the gas pipeline of the length of almost 7.50 m was completely flooded with water. The sections flooded with water were also found in other areas of the network system (Fig. 1).

Figure 1. *Cutting of the DN300 gas pipeline at Myśliwska Street in Kołobrzeg*

The analysis of the causes of the incident from the side of the gas plant was conducted only in one direction – the search for a potential place of leakage which would allow for penetration of such quantity of water into the gas pipeline from the outside. Such a place was not found until these gas pipelines were replaced with new polyethylene ones. Therefore, the thesis that water got into the gas pipeline through the places of leakage has never been proved unambiguously.

We may also refer here to the case of the famous accident that took place in Zielona Góra on 30 November 2010. Then, as a result of a failure of the gas reduction system, the medium-pressure gas penetrated into the low-pressure housing estate gas network at three housing estates, causing an explosion of flats and fires [10]. The analysis conducted by the public prosecutor's office proved that

one of the main factors of the failure was undoubtedly water which froze in the devices and pipes of the gas station regulation and safety systems. However, the experts decided *a priori* that it was water from precipitation. No observations and studies in this direction were undertaken. Again, the prevailing stereotype that the natural gas is a dry gas, as highlighted in this article, worked.

Experiment conditions and experimental studies results

All analyses and research in the field of natural gas humidity have always concerned the area of mines, high-pressure transit gas pipelines and – to lesser extent – medium-pressure gas networks. The current water protection system ends with dehydrators installed as a standard on the inlet systems of the medium-pressure gas stations. There is no data on the study of this phenomenon at the side of the low-pressure network, i.e. directly in front of the consumer. As it has already been said, there are currently no provisions requiring the use of the dehydrators in the low-pressure systems as well.

The author's analysis of a number of failures has showed that the low-pressure systems may contain water, the presence of which cannot be explained by leakages or penetration of precipitation into the network. Therefore, it has been decided to carry out an analysis of the water content in the low-pressure natural gas that is supplied directly to the customers. The local gas network system in the Kołobrzeg zone distributing the medium-pressure L_s subgroup gas with subsequent reduction to 1.3 kP pressure was selected for the study. The point, at which the sampling was carried out, was at a household customer supplied directly from the medium-pressure gas network. The low pressure is obtained thanks to a household gas regulator, which only has a standard inbuilt tissue filter. Such conditions of the experiment allowed for examination of the moisture content after leaving of the high-pressure station and before passing through the dehydrators at II° gas stations.

The measurements were carried out with the use of XENTAUR portable dew point analyser, HPDM type (Fig. 2). It is a microprocessor-controlled, battery-powered moisture meter, equipped with a dry chamber for storage of the sensor. This allows for obtaining of a reliable result after moving of the sensor to the measuring cuvette, ensuring the maximum possible tightness and the lowest possible gas exchange between two chambers during the sensor movement.

FIGURE 2. *XENTAUR moisture meter, HPDM type*

The thermodynamic calculations allow for calculation of the experimentally obtained dew point temperature value based on the known conditions in the higher-pressure gas pipelines. The generally accepted principles of such recalculation are based on the Goff-Gratch formula or on a similar method of the World Meteorological Organization. In the work, the JSC Ecological Sensors and Systems humidity calculation software [2], which allows for comparison of the results according to both methods and for changing of the type of the analysed gas, has been used. Both the measured values and the ones obtained as a result of such calculations are presented in Table 1.

TABLE 1. *Natural gas humidity measurement and recalculation results*

Date of measurement	Dew point temp., °C	Gas humidity, g/m³	Recalculation into medium-pressure conditions			Recalculation into high-pressure conditions		
			Pressure, MPa	Dew point temp., °C	Gas humidity, g/m³	Pressure, MPa	Dew point temp., °C	Gas humidity, g/m³
25.06.19	–29.4	0.322	0.298	–16.1	4.36	4.2	16.4	46.42
06.06.19	–22.1	0.66	0.292	–7.7	13.84	2.5	19.1	88.83
20.06.19	–25.5	0.461	0.297	–11.9	9.92	4.23	22	83.53
21.05.19	–27.5	0.385	0.293	–14.4	9.75	4.22	18.7	104.33
22.05.19	–27.7	0.366	0.293	–15.2	12.56	4.19	17.5	133.38
13.06.19	–25.8	0.362	0.296	–14.8	6.9	4.2	17.9	72.94
21.06.19	–27.9	0.362	0.298	–14.9	8.25	4.21	17.7	86.76
23.06.19	–28.1	0.351	0.294	–15.7	10.62	4.15	16.8	112.05
21.06.19	–28.2	0.35	0.298	–15.4	6.61	4.3	17.7	72.2
01.07.19	–28.3	0.35	0.297	–15.4	6.98	4.1	16.9	72.91
01.09.19	–28.3	0.344	0.296	–15.4	4.89	4.02	16.7	50.13
26.06.19	–28.5	0.34	0.297	–15.5	4.59	4.13	16.9	48.19
24.06.19	–28.7	0.331	0.299	–16	6.84	4.31	16.8	74.61
24.05.19	–28.8	0.329	0.294	–16.3	7.12	4.22	16.3	76.95
06.08.19	–28.9	0.327	0.297	–16.2	6.17	4.02	15.6	63.07
27.06.19	–28.9	0.325	0.298	–16.3	7.31	4.02	15.3	74.56
02.07.19	–29.2	0.316	0.298	–16.8	8.24	4.29	15.8	89.68
21.08.19	–29.4	0.305	0.3	–17	6.51	4.25	15.3	69.78
22.06.19	–29.9	0.293	0.299	–17.6	6.61	4.09	14	68.39
16.06.19	–30	0.289	0.298	–17.8	6.9	4.21	14.2	73.63

Measurement conditions: t = 22°C, p = 1.13 kPa ($p_{abs.}$ = 0.102625 MPa).

The Table 1 data shows that the gas with a very low dew point temperature is formally transported through the low-pressure network. On the other hand, the recalculations into the medium- and high-pressure conditions show that the same water vapour content before pressure reduction does not exclude the possibility of water condensation in the domestic climate conditions. The performed analysis of the reports on the supervision over the dehydrators located on the high-pressure network in the Gas Plant in Koszalin, conducted in the period from January 2016 to December 2019, showed that water was pumped out from the dehydrators in the quantity of about 3.700 litres. The maximum quantity of water utilised from one dehydrator was 375 l.

The failures analysed above show that in the conditions of higher pressures and high gas velocities, penetration of liquid water through the dehydrators and then through the reduction station equipment into the low-pressure network cannot be excluded.

Summary

In the recent years, along with development of the polyethylene pipe technology, a growing tendency to move away from the old principles for designing and construction of the gas networks, proved over the years, has been observed. The declines of the laid gas pipelines are only forced naturally by the fall of the terrain and upon the repairs and replacements of the steel network with the PE one, the old dehydrators are massively removed at the lowest points of the network. In most cases, this does not cause problems in the further operation, even if in such a system a part of the network is already made of polyethylene pipes and a part is still made of steel. But usually these are the systems supplied by the *E* subgroup gas, where the main supplier seeks the permissible moisture content in the gas. It is bound by the supply agreement specifying the maximum dew point temperature value.

The situation is different in the systems supplied by the L_w or L_s subgroup gas from the local mines.

The changing designing trends result in the fact that the dehydrators are less and less installed on the networks. The suddenly appearing water, causing failures, surprises the employees of the gas plants, who are unable to explain the reasons for this phenomenon.

This is what happened in the case of the analysed failure in Kołobrzeg. At that time, the use of the dehydrators during construction of passages under the tracks was definitely required due to greater deepening with creation of a natural trap. However, this requirement was omitted during network modernisation.

Appropriate conclusions were drawn only after the failure. Figure 3 shows the dehydration system prepared for installation during replacement of three sections of the gas pipelines running under the tracks with a new PE gas pipeline with the main diameter DN 355 mm upon the request of the network operator in Kołobrzeg.

Figure 3. *Polyethylene dehydrator with diameter DN 355 (without inspection pipe)*

Conclusions

1. The research results presented in the article prove that water condensation in the higher-pressure networks, having the consequence of penetration through the I° and II° reduction stations, may be the source of significant quantities of water in the low-pressure networks. No studies have proved or excluded the possibility of water entering directly the low-pressure gas pipelines through leakage places.
2. The analysed failures prove that regardless of the source of water, it is unjustified to dispose of the dehydrators, especially in a mixed gas network made of polyethylene and steel pipes distributing the gas from the local wells of the L_w and L_s subgroups.
3. The target action would be to introduce appropriate changes to the "Rules for designing n of low- and medium-pressure steel gas pipelines and polyethylene gas pipelines" and the Regulation of the Minister of Economy of 26 April 2013 "On technical conditions to be met by gas networks and their location" in terms of introduction of the legal conditions relating to the possibility or necessity to use the dehydrators in the specific cases.

Conflicts of Interest: The author declares no conflict of interest.

References

[1] Grynia E., Carroll J., *Niepożądana woda, czyli przegląd procesów osuszania gazu ziemnego*, Szejk, październik 2013, PGNiG, pp. 18-23.

[2] *Humidity units conversion utility*, 2019, https://www.eksis.ru/technical-support/humidity-calculator.

[3] Kolass R., Parker C., *Moisture measurement in natural gas*, The International Instrumentation and Control Engineering Website, 2015, http://www.iceweb.com.au (date accessed: 18.06.2015).

[4] Polish standard PN-C-04752 (2011-1). Natural gas – Gas quality in the transmission network.

[5] Polish standard PN-C-04753 (2011-2). Natural gas – The quality of gas supplied to customers from the distribution network.

[6] Polska Spółka Gazownictwa. Development Strategy for 2016 – 2022, https://www.psgaz.pl/documents/21201/329214/Strategia+PSG+2016+-+2022.pdf/a95241fa-85d1-4ee6-8de7-906792e30cb4.

[7] Draft of the Energy Policy of Poland to 2040 (PEP2040, rev. 2.1 of 08 November 2019) https://www.gov.pl/web/aktywa-panstwowe/zaktualizowany-projekt-polityki-energetycznej-polski-do-2040-r.

[8] Recknagel H. et al., *Ogrzewanie i klimatyzacja*. *Poradnik*, EWFE, Gdańsk 1994.

[9] Szkarowski A., Janta-Lipińska S., Kolienko A., *Kontrola jakości gazu narzędziem oszczędzania energii*, Gaz, Woda i Technika Sanitarna, Nr 4, 2013, pp. 146-150.

[10] Shkarovskiy A., Kotuła M., *Accident Analysis of Low Pressure Gas Distribution Systems*, Architecture and Engineering, Vol. 3, Issue 4, 2018, pp. 42-48.

Hanna KOSHLAK, Anatoliy PAVLENKO
Kielce University of Technology, Poland

Doi: 10.53412/jntes-2020-4.3

THERMOPHYSICAL PROPERTIES OF POROUS MATERIALS

Abstract: *The study of the porosity of thermal insulation made of refractory materials is an important task for the power industry, since the thermal conductivity of porous materials depends on the shape and especially the location of the pores. An analytical review of existing technologies shows that research in this area is not enough to simulate the process of heat and mass transfer in porous alumina material. Experimental determination of the characteristics of heat and mass transfer in porous materials during the formation of a porous structure is a pressing scientific problem. This article analyzes the influence of the composition of materials on the formation of pores, as well as the effect of various impurities and temperature on the thermal conductivity of the material.*

Keywords: *porous materials, composite insulation materials, alkaline silicate, thermal bloating.*

Statement of the problem

Investigation and control of the processes of structure formation of materials are difficult tasks, which are still unsolved. Clear understanding of the mechanism of structure formation makes it possible to develop a methodological basis of new technologies, including the technology of production of thermal insulating materials with predictable thermal properties.

However, the ways of formation physical properties of the material were not found. A lot of experimental data show the relationship between the porosity of the material and its thermal properties [7, 9, 13]. It is obvious that the structure of the materials, in particular the porosity, determines their properties. But in the mentioned works this impact is shown in different ways. For example, in the [13] the thermal conductivity of Fe (58.19 W/(m·K)) and of clay (3.26 W/(m·K)) differ by 18, but the thermal conductivity of insulation structures, which are made from granules of Fe and granules of clay with the same porosity are almost equal – 0.0403 W/(m·K) and 0.0402 W/(m·K). Such results show that not only porosity, but also size and shape of the pores affect the properties of the material. Since any material has an own characteristic distribution of the pore size, it is obvious that various researchers obtained conflicting information about the nature of the influence of pore size on the thermal properties of these materials. Current technologies of structure formation do not provide the prediction of the geometric structure, which means that there is no possibility to predict the properties of materials.

Literary analysis and the problem statement

In [4, 7, 9, 13] the dependence of the thermal properties of porous materials on a structure was discussed, but recommendations about optimal structure were not given. In [2, 3, 5] the dependence of the mechanical properties on a structure of porous materials was analyzed and recommendations about structure formation with predicted properties were given, but there was no information about the thermal properties.

In [6] the influence of internal pore pressure on closed-cell elastomeric foams was explored. Changes of internal pore pressure with different hydrostatic loads were considered. Obtained results show that this pressure can significantly change macroscopic reaction and stability of closed-cell elastomeric foams. Also it shows that elastomeric foams with internal pore pressure have a higher stiffness, even with atmospheric pressure, than without it. But the method of calculating the internal pore pressure was not given. Also pressure was taken only as a function of density. In [14] changes of the structure with a closed porosity under compression and extension, with different initial pressures in the pores, were researched. Experiment results show, that internal pressure has a positive effect under compression and negative under extension. The impact of deformation on the structures with closed porosity can lead to high initial pressure in the pores, which increases the total energy absorption and stiffness of the material under the process of deformation. But nothing was said about the methods of achieving certain pressure in the pores of the material and its calculation.

In [1] the micromechanical analysis of the porous material with internal pressure in the pores was made, the polymer BX-265 was taken as experimental material. The influence of initial pore pressure on the predicted elongation of the sample and the influence of the applied load (with pressure in the pores and without it) on the predicted break of the sample were shown. But nothing was said about the calculation methods of internal pore pressure.

In [12] the dependencies of thermal characteristics from the structure of materials were compiled and the task of the controlled pore formation by adjustable heat treatment of the raw gel-like mixture was formulated. In [8, 10, 11] the main physicochemical formation processes of the gas-vapor area (pores) were analyzed, which were taken as a basis in this work.

All mentioned works have one main idea that materials structure affects their properties. But there are no practical recommendations about formation of specific material structure.

Above information cannot be generalized, because it's contradictory. That's why existing technologies of the thermal swelling (structure formation) can't give the required structure.

The purpose and objectives of the research

The purpose of this work is the research of regularities of gas-vapor phase formation in liquid mixtures, which are in a state of thermodynamic equilibrium.

To achieve this purpose, next objectives must be solved:

- to simulate the condition of thermodynamic phase equilibrium in the liquid mixture to control the process of pore formation;
- to determine the energy parameters of the swelling process (the pressure of the pore former agent gas inside the closed spherical pore, the conditions of thermal balance);
- to determine the overheating temperature of the liquid mixture to assess the growth dynamics of the gas-vapor area;
- to research the growth dynamics of the gas-vapor phase (pores).

Materials and methods of research

Carrying out the practical research into raw mass, we added the chamotte clay or pure structural clay, the composition of which is shown in the Table 1.

The research was performed by the use of differential thermal analysis (DTA) of the thermal bloating process for the raw mixture.

TABLE 1. *The chemical composition of fire-clay*

No.	Clay	The content of oxides, %									
		SiO_2	Al_2O_3	Fe_2O_3	TiO_2	CaO	MgO	K_2O	Na_2O	SO_3	Lost on ignition
1.	Structural clay	44.59-54.14	27.13-35.85	1.48-2.47	1.14-1.97	0.38-0.81	0.23-0.42	0.21-0.60	0.25-0.45	1.34-3.62	11.48-13.86
2.	Chamotte clay	46.80	36.80	1.58	–	0.20	0.76	0.34	0.18	–	13.6

Trails are performed at a constant rise of temperature with recording the temperature difference on the chart paper as a function of temperature. The result is a curve DTA (Figs. 1-4). At processing the experiment's results, the horizontal axis should be graded by temperature. According to the position of peak of the endothermic process, the temperature interval of phase transitions can be found.

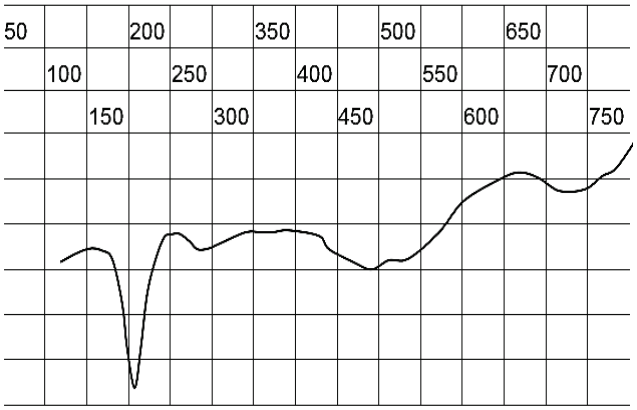

FIGURE 1. *DTA of raw material mixture with a content of 75 mass fractions of clay No. 1 (Table 1)*

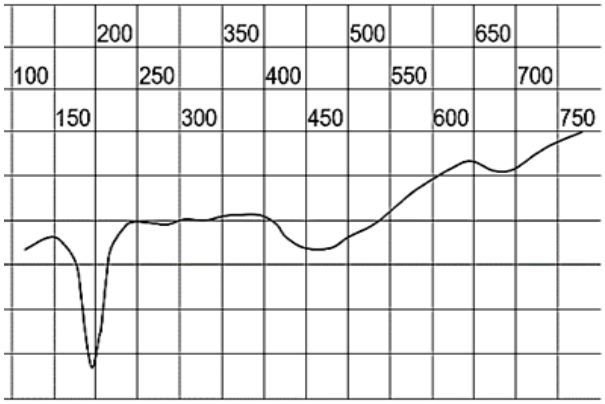

FIGURE 2. *DTA of raw material mixture with a content of 75 mass fractions of clay No. 2 (Table 1)*

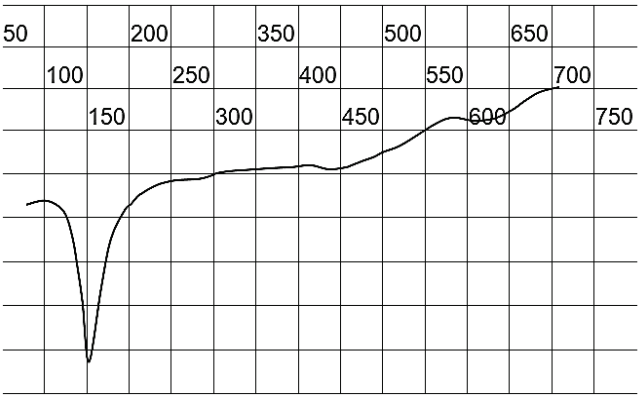

FIGURE 3. *DTA of raw material mixture with a content of 160 mass fractions of clay No. 1 (Table 1)*

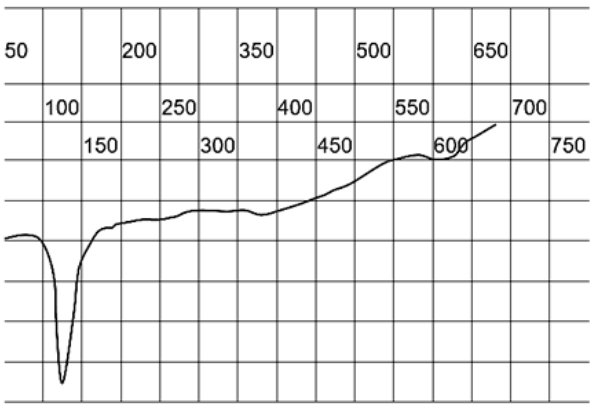

FIGURE 4. *DTA of raw material mixture with a content of 160 mass fractions of clay No. 2 (Table 1)*

Changes, which had the place during the heating, showed three endothermic effects: 146, 450, and 720. A large endothermic effect due to the removal of absorbed water is at 146°C, and the observed step at 300°C on the curve says about removal of interpacket water. The second effect (450-550°C) corresponds to the removal of the constitutional water (bound into the form of OH). The endothermic effect at 720°C, it explains the removal of OH-ions. As it can be seen from the data chart, the optimum temperature range for dehydration of the mixture is within 146-720°C. It should be defined the connection of temperature intervals with the structure of bloated material, and, consequently, with the

useful application properties (strength, conductivity, heat resistance, water absorption). For this, changing the composition of the initial mixture, the measurements were repeated under method presented above.

On the obtained DTA curves for all experimental samples in the investigated temperature intervals a number of phenomena associated with thermal effects is observed:

- up to 100°C – evaporation of chemically unbound water;
- 100°C, ..., 170°C – a sudden loss of mass and strongly expressed endothermic effect that is related to the partial dehydration of gel and phases of different composition;
- 450°C, ..., 550°C – endothermic effect that corresponds to the decomposition of portlandite with water vapor emission;
- 700°C, ...,900°C – a minor loss of mass and weak endothermic effect, which is related to the decomposition of carbonate minerals (calcite, dolomite), and late-stage dehydration of gel and hydro aluminates.

The morphology and porosity of the samples were determined by optical methods. According to this method, the macroscopic parameters of porosity inside metric interval with a lower bound of 10 mμ and upper bound of 5 mm are determined. The specified interval characterizes the strength parameters of the substance and parameters of heat and mass transfer.

The characteristic feature of the obtained data is that graphs for different types of clay are almost the same. Significant differences are in reading for different temperature minimums. So, for the first endothermic minimum, we received the bloated material with small and almost spherical pores [2, 6]. Most of them had a minimum size. The bloating of the raw material mixture in the second endothermic minimum provides a mixed porosity (spherical cellular and channel). The material becomes less solid. When there is bloating in the conditions of the third endothermic minimum the channel porosity is mainly formed. This material has the lowest strength. You should expect the reducing in thermal conductivity with increasing temperature of bloating.

The obtained material has a low thermal conductivity even at temperatures of 1000-1200°C (Fig. 1). The thermal conductivity of the material was determined by thermal conductivity meter IT – λ – 400. Samples with a cylindrical form (height 5 mm, diameter 15 mm) were put inside the meter and were processed by temperature influence from 200°C to 700°C.

In this temperature range, the thermal conductivity of the material was determined according to the standard method, which is described in the device manual.

Figure 5 shows the experimental dependence of thermal conductivity on the temperature of the material, for technologies of which the main technological stages were simulated.

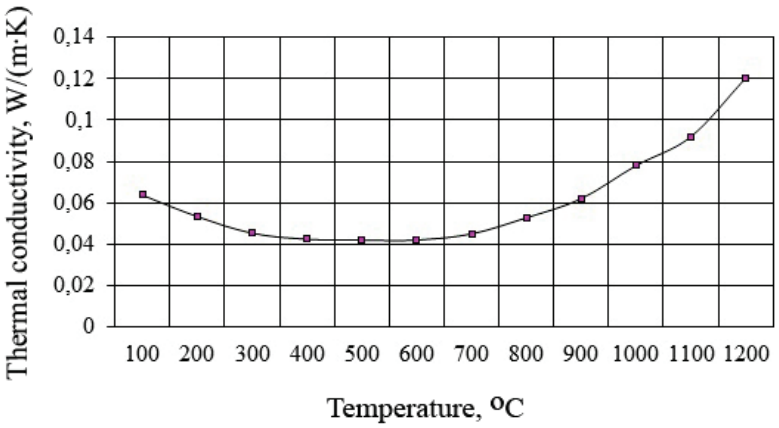

FIGURE 5. *Dependence of thermal conductivity on the temperature*

Equilibrium conditions of the pore agent in the material, during the formation of the porous structure

As the dynamic characteristic, which determines the direction of size changes in vapor pore, tension difference was taken, which was caused by the pressure in the vapor area and by the resistance of the boundary surface of the pore. The equation, which characterizes the dynamics of growth or reduction of the vapor bubble [12]:

$$\frac{dw}{d\tau}=-\frac{1.5\rho w^2+P_g-P_n(T)}{\rho_g R}=-\frac{1.5\rho w^2}{\rho_g R}+\frac{P_n(T)-P_g}{\rho_g R} \tag{1}$$

where:

w – speed of growth of the vapor bubble;

τ – time of bubble growth;

ρ – density;

P_g – pressure inside the vapor area;

P_n – pressure in the surrounding liquid;

T – temperature;

R – radius of the vapor bubble.

Increasing, decreasing and stabilization of the bubble sizes can be represented by three cases:

$$\begin{cases} w=\dfrac{\alpha\left[\left(w_0-\alpha\right)e^{-\frac{1.5\rho\tau}{\rho R}}+w_0+\alpha\right]}{w_0+\alpha-\left(w_0-\alpha\right)e^{-\frac{1.5\rho\tau}{\rho R}}}; \\ \alpha=\sqrt{\dfrac{P_n(T)-P_g}{1.5\rho}}; \\ \dfrac{P_n(T)-P_g}{1.5\rho}>0; \\ w=\dfrac{\sqrt{\left|\dfrac{1.5\rho}{P_n(T)-P_g}\right|}w_0-\operatorname{tg}\dfrac{\rho\tau}{\rho_g R}}{\sqrt{\left|\dfrac{1.5\rho}{P_n(T)-P_g}\right|}+\left|\dfrac{1.5\rho}{P_n(T)-P_g}\right|w_0\operatorname{tg}\dfrac{\rho\tau}{\rho_g R}};\ \dfrac{P_n(T)-P_g}{1.5\rho}<0; \\ w=\dfrac{w_0\rho_g R}{1.5\rho w_0\tau-\rho_g R}; \\ P_n(T)-P_g=0 \end{cases} \tag{2}$$

In the last case, when $P_n(T)-P_g=0$ – the gas-vapor area (pore) doesn't change in volume. In the technological aspect, relations between energetic parameters, which characterize the predicted pore size (average), were achieved. Therefore, thermophysical parameters also were achieved, including thermal conductivity.

The equation for finding the speed of size changing of the pore, can be written as:

$$\frac{dR}{d\tau} = \frac{w_0 \rho_g R}{1.5 \rho w_0 \tau - \rho_g R} \tag{3}$$

where w_0 is the initial velocity of the boundary of the vapor region (accept 1).

When solving the equation (3), duration of the swelling process can be found. Since the average value of the pore size is one of the main factors, which determine thermophysical properties of the sample, it this method gives a chance to predict the discussed properties (Fig. 6).

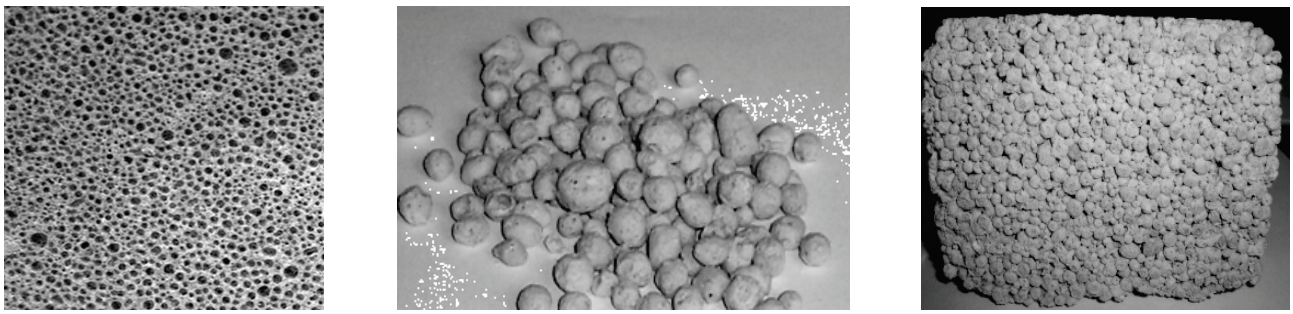

D = 3-6 mm

FIGURE 6. *New materials for thermal protection of buildings*

Conclusions

The solution of creating new porous thermal insulation materials and technologies of their production is inextricably related to scientific research in energy transferring of porous structure during the stages of bloating, hardening and drying under the condition of providing the lowest thermal conductivity and density.

The indicated material properties are determined by a rate of their porosity, the ratio of micro and macro porosities, properties of interporous material that form a kind of supporting structure, which in its turn is determined by the production technology, type of raw materials and conditions of their preparation. All mentioned above impose the special requirements to the formation of material structure to ensure its relatively high strength and durability.

With the help of differential thermal analysis, the modes of heat treatment have been studied; the rational parameters of thermal bloating has been defined that allows to implement the process with minimal energy consumption and the predicted thermal properties of obtained materials.

Conflicts of Interest: The author declares no conflict of interest.

References

[1] Aboudi J., Arnold S.M., Bednarcyk B.A., *Micromechanics of Composite Materials: Generalized Multiscale Analysis Approach*, Elsevier, 2013, p. 973.

[2] Bajare D., Kazjonovs J., Korjakins A., *Lightweight Concrete with Aggregates Made by Using Industrial Waste*, Journal of Sustainable Architecture and Civil Engineering, Vol. 4, Issue 5, 2013, doi: 10.5755/j01.sace.4.5.4188.

[3] Eom J.-H., Kim Y.-W., Raju S., *Processing and properties of macroporous silicon carbide ceramics*, Journal of Asian Ceramic Societies, Vol. 1, Issue 3, 2013, pp. 220-242, doi: 10.1016/j.jascer. 2013.07.00.

[4] Freire-Gormaly M., *The Pore Structure of Indiana Limestone and Pink Dolomite for the Modeling of Carbon Dioxide in Geologic Carbonate Rock Formations*, Department of Mechanical and Industrial Engineering University of Toronto, 2013, available at: https://tspace.library.utoronto.ca/bitstream/1807/42840/1/Freire-Gormaly_Marina_201311_MASc_thesis.pdf.

[5] Komissarchuk O., Xu Z., Hao H., *Pore structure and mechanical properties of directionally solidified porous aluminum alloys,* China Foundry, Vol. 11, Issue 1, 2014, pp. 1-7, available at: https://doaj.org/article/002c72e2e01345db8bf4fef190113057.

[6] Lopez-Pamies O., Ponte Castañeda P., Idiart M.I., *Effects of internal pore pressure on closed-cell elastomeric foams*, International Journal of Solids and Structures, Vol. 49, Issue 19-20, 2012, pp. 2793-2798, doi: 10.1016/j.ijsolstr.2012.02.024.

[7] Nimmo J.R., *Porosity and Pore Size Distribution*, Encyclopedia of Soils in the Environment, Elsevier, London 2004, pp. 295-303.

[8] Pavlenko A.M., *Dispersed phase breakup in boiling of emulsion*, Heat Transfer Research, Vol. 49, Issue 7, 2018, pp. 633-641, doi: 10.1615/HeatTransRes.2018020630.

[9] Pavlenko A., Koshlak H., *Production of porous material with projected thermophysical characteristics*, Metallurgical and Mining Industry, Vol. 1, 2015, pp. 123-127.

[10] Pavlenko A., Koshlak H., *Design of the thermal insulation porous materials based on technogenic mineral fillers*, Eastern-European Journal of Enterprise Technologies, Vol. 5, No. 12 (89), 2017, pp. 58-64.

[11] Pavlenko A., Koshlak H., Slowak A.M., *The use of the ash of thermal power plants for the production of efficient porous insulation*, E3S Web of Conferences 86, 00003, Vol. 86, 2019, doi.org/10.1051/e3sconf/20198600003.

[12] Pavlenko A., Szkarowski A., *Thermal insulation materials with high-porous structure based on the soluble glass and technogenic mineral fillers*, Rocznik Ochrona Środowiska, Vol. 20, Issue 1, 2018, pp. 725-740.

[13] Shpac A., Cheremskoj J., Kunickij O., Sobol, *Clasters nanostrukturnye materials*, Poristost 'as a special state samoorganizovannoi structure in the solid state and materials, Akademperiodika, Vol. 3, Kyiv 2005, p. 516.

[14] Vesenjak M., Öchsner A., Ren Z., *Influence of pore gas in closed-cell cellular structures under dynamic loading*, German LS-DYNA Forum, Bamberg 2005, available at: https://www.dynamore.

Alexander DRYUCHKO
Dmitriy STOROZHENKO
Natalia BUNYAKINA
Irina IVANYTSKA
Alexander KULCHIY
Dmitriy GOLUBATNIKOV
Poltava National Technical University Named in Honor of Yuri Kondratyuk, Ukraine
e-mail: dog.chemistry@mail.ru

Doi: 10.53412/jntes-2020-4.4

PHYSICO-CHEMICAL ASPECTS OF USING REE-CONTAINING NITRATE SYSTEMS IN FORMING MULTICOMPONENT OXIDE FUNCTIONAL MATERIALS

Abstract: *For obtaining the nanosized inorganic materials on oxides of transition and rare earth elements, the most promising is the use of methods of "soft chemistry" based on synthesis from aqueous or non-aqueous solutions at relatively low temperatures. Their key advantages are: the possibility of obtaining products with controlled composition and micromorphology, efficiency, environmental acceptance and so on.*

Keywords: *nanoscale materials, properties of bulk materials, inorganic materials on oxides.*

Statement of the problem

Considerable attention that now is being paid to the study of nanoscale materials, primarily, is due to significant differences of their properties from the properties of bulk materials of the same composition and is the result of detection by them of quantronix effects.

Unfortunately, the vast majority of the currently known studies does not make it possible to formulate general principles for creation of nanomaterials possessing the assigned composition, micro- and mesostructure, functional characteristics. The main reason for this is that the mechanism of nanoparticles formation in these conditions is rather complex from physico-chemical point of view and may include parallel processes of hydration (solvation), association, complexation, formation and transformation of heterophases, laws of which are poorly understood. In this regard, one of the main challenges in the development of reproducible methods for the directed synthesis of nanodispersed materials using approaches of "soft chemistry" is a detailed study of mechanisms and dynamics of processes taking place during formation of nanoparticles. Such fundamental study envisages a systematic study of the composition and micromorphology of intermediate compounds, that in most cases determine the microstructure and structure-sensitive characteristics of the final functional nanomaterials.

Modern REE oxides-containing functional materials are extremely diverse. A common uniting point for all of them is the structure. Transition metals in structure of complex oxides coordinate oxygen poledra of different configurations. The structure of substances is formed by various combinations between polyhedra, which in different combinations can be united by vertices, edges, faces. In cavities formed by fragments of polyhedra rows the larger cations of alkali, alkaline earth, rare-earth elements are placed. Many properties of complex oxides depend not only on their composition and structure but also on defect structure that purposefully allows to influence their target parameters.

At present, the search of new methods and complex technologies for the synthesis of special, functional REE oxide-containing materials with a liquid multi-component nitrate systems [1-15] is being carried out. Such technological schemes are based on the production of fine powder materials by chemical homogenization of initial components in joint selection of products from the liquid phase by sequential or joint deposition followed by heat treatment in the form of their hydroxides or other insoluble compounds; the use of a thermolysis method of a solvent, ionic and molecular coordination precursors; replacement of a solvent; a spray drying; cryochemical crystallization, sol-gel processes, etc. The synthesis of nanocrystalline materials is a complex scientific and technological problem.

The information about the condition [15] and possible ways of improvement of creation technologies of REE oxide-containing functional materials is available [16], the existing requirements to their stability and reproducibility properties initiated our study.

Problem formulation and solution methods

The aim of this work is a basic research of cooperative processes proceeding upon obtaining the oxide rare earth-containing functional materials using nitrates of elements of various electronic structure and finding the possible methods of influence on liquid-phase and solid-phase systems based on thermal activation of reagents for reproducing their structure-sensitive characteristics. In the work to assess the management of these processes and to obtain materials with the desired properties as model it was studied the system KNO_3-Nd-$(NO_3)_3$-H_2O, components of which specify the technical characteristics of the synthesis product or modify its physical properties. The choice for studies of neodymium nitrate (as representative of the rare earth elements of cerium subgroup) is determined by existing statistical data about the most probable changes in composition or structure of the compounds created by neodymium while passing from lanthanum to lutetium in a natural number. The choice of values for the temperature section 50°C for studying the solubility isotherms of the system is determined by instability of hexahydrate of neodymium nitrate and start point of its melting in crystalization water at 68°C, above which it is in a liquid highly viscous metastable condition.

To solve this problem, our research were focused on:

- solid analytical literature review of the available scientific information on the subject of the work;
- the choice of methods and means of physico-chemical studies of a model system;
- mastering the methods and techniques of preparation and conduct of the experiment;
- experimental study of chemical interaction of components, heterogeneous equilibria in water-salt system KNO_3-Nd-$(NO_3)_3$-H_2O (50°C) with the application of complex physico-chemical methods;
- building the isothermal solubility chart system. Determination of concentration limits of original compounds crystallization and identified of complex salts in the system;
- identification of optimal growth conditions and performing the synthesis of coordinating neodymium nitrates and potassium examination of their properties and confirmation of identity;
- thermographic study of solid phases produced in the system of neodymium nitrate and potassium from solutions, solutions – melts, melts;
- clarification the nature and peculiarities of sequential thermal transitions in the rare earth-containing nitrate multicomponent systems in different aggregate states during the heat treatment;
- using the acquired knowledge to justify the preparatory processes in the production of REE-containing functional materials for various purposes, development of possible ways to control them.

To clarify the nature of chemical interactions and phases equilibria in water-salt system of the studied nitrates (precursors of multicomponent oxide functional materials) in full concentration ratios in a temperature range of solutions existence the method of solubility, described in [17, 18], was used.

The method allows to find the limits of self-development, to which in specific conditions in equilibrium state the isolated system of this composition aims.

The transformations nature of solid phases, crystallizing in the investigated ternary system was studied using the method of thermal analysis on derivatograph Q – 1500 D, the developed thermoanalytical complex, as well as methods of elemental and X-ray analysis.

The experimental part

In this work as source salts there were used hydrated and anhydrous nitrates of these elements of the brand „p.f.a.", additionally purified by recrystallization.

Heterogeneous equilibria in aqueous system of nitrate salts was studied isothermally at 50°C in dry air thermostat, with continuous mixing using the mixing electromagnetic multi-device. The equilibrium of phases was established within 1-2 days. Sampling of liquid and solid phases of the investigated mixtures for preventing crystallization and maximum separation of mother mix were carried out by a special samplers in the same isothermal conditions using the forvacuum pump.

The chemical analysis of liquid and solid phases, the „leftovers", were tested on the content of Nd^{3+} ions, they were determined trigonometrically; ions K^+ were calculated according to the difference concerning the total content of nitrates in dry residue. The obtained experimental data from the studied system for individual ions were calculated according to their salt content, generalized, summarized in Table 1 and according to the correspondent principles were applied to the solubility chart (Fig. 1). Graphical display of composition of solid phases formed in the system was carried out according to Schreinemakers [17, 18]. Their identity was confirmed by chemical, X-ray phase, thermal and other methods of analysis.

The study of mutual behavior of structural components in a liquid phase and phase of equilibria in the system of potassium nitrate-neodymium nitrate-water, the building of its solubility isotherms allow to determine the concentration boundaries of separation into the solid phase of potassium coordinating neodymium nitrates. The obtained data allowed to make the choice of optimal conditions of separation of complex nitrates and carry out their synthesis by isothermal evaporation of the solvent. In slightly supersaturated mother mixture isometric crystals of binary potassium nitrates were obtained. The habitus of crystals $K_2[Nd(NO_3)_5(H_2O)_2]$ (Fig. 2a), $K_3[Nd_2(NO_3)_9]\cdot H_2O$ (Fig. 2b) is determined by the composition of compounds, the nature and content of their constituent cations, conditions of crystallization and is their diagnostic sign.

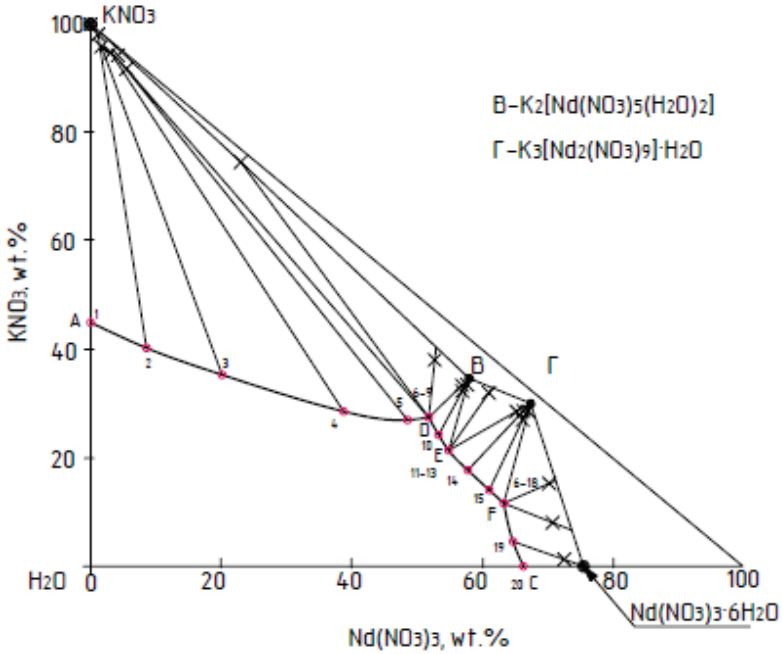

FIGURE 1. *Solubility system isotherm KNO_3-$Nd(NO_3)_3$-H_2O at 50°C*

Table 1. *Data of phase equilibria study in the system KNO_3-$Nd(NO_3)_3$-H_2O at 50°C*

Points of composition	Saturated solution				Composition of "leftovers", wt. %		Solid phases*
	Composition, wt. %		Properties				
	KNO_3	$Nd(NO_3)_3$	$d \cdot 10^3$ kg/m^3	*n*	KNO_3	$Nd(NO_3)_3$	
1	2	3	4	5	6	7	8
1 A	44.88	0.00	1.223	1.3748	100.00	0.00	A
2	40.12	8.67	1.391	1.3862	97.93	1.25	Also
3	35.21	20.31	1.514	1.4014	95.68	1.72	–
4	28.46	38.81	1.602	1.4406	94.51	3.22	–
5	26.80	48.65	1.858	1.4659	94.03	4.36	–
6					91.54	5.56	–
7					74.51	23.07	A + B
8 D	27.26	51.82	2.092	1.4781	37.95	52.73	Also
9					33.84	56.49	B
10	24.08	53.28	2.064	1.4764	34.07	57.16	Also
11					34.58	57.29	–
12 E	21.34	54.91	2.068	1.4791	31.95	60.97	B + F
13					29.82	65.46	F
14	17.03	57.09	1.960	1.4772	30.12	66.91	Also
15	13.94	61.08	1.969	1.4778	29.23	66.65	–
16					29.61	67.07	–
17 F	11.49	63.31	2.124	1.4822	15.17	70.18	F + G
18					8.01	70.76	Also
19	4.44	66.02	1.964	1.4726	1.76	72.49	G
20 C	0.00	66.16	1.974	1.4667	0.00	75.28	–

* A – KNO_3; G – $Nd(NO_3)_3 \cdot 6H_20$; B – $K_2[Nd(NO_3)_5(H_2O)_2]$; F – $K_3[Nd_2(NO_3)_9] \cdot H_2O$.

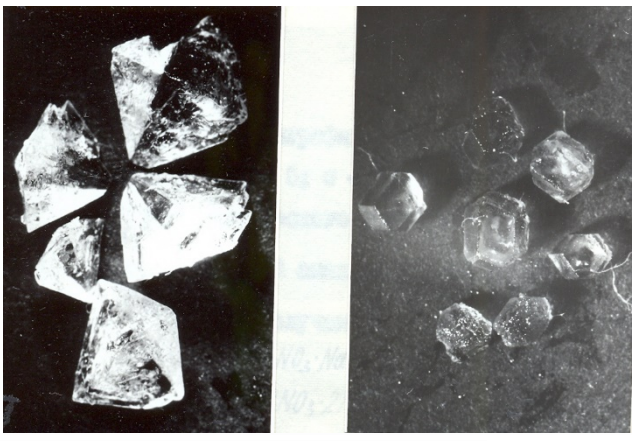

a) *b)*

Figure 2. *Microphotoes of crystals: a) $K_2[Nd(NO_3)_5(H_2O)_2]$; b) $K_3[Nd_2(NO_3)_9] \cdot H_2O$*

The chemical analysis of the synthesized compounds confirms the mass ratio of elements in the above formulas. The conducted X-ray phase analysis of samples indicates that the compounds are characterized by individual set, position and intensity of lines in the diffraction charts (see Fig. 3) and it confirms their individuality. Thermographic examination of initial nitrates KNO_3, $Nd(NO_3)_3 \cdot 6H_2O$; solid phases formed in the system of neodymium nitrates and potassium; synthesized potassium coordinating nitrates of REE were conducted on the developed thermoanalytical complex for differential thermal analysis and on derivatograph of F. Paulik, I. Paulik, L. Erdei Q – 1500 D system.

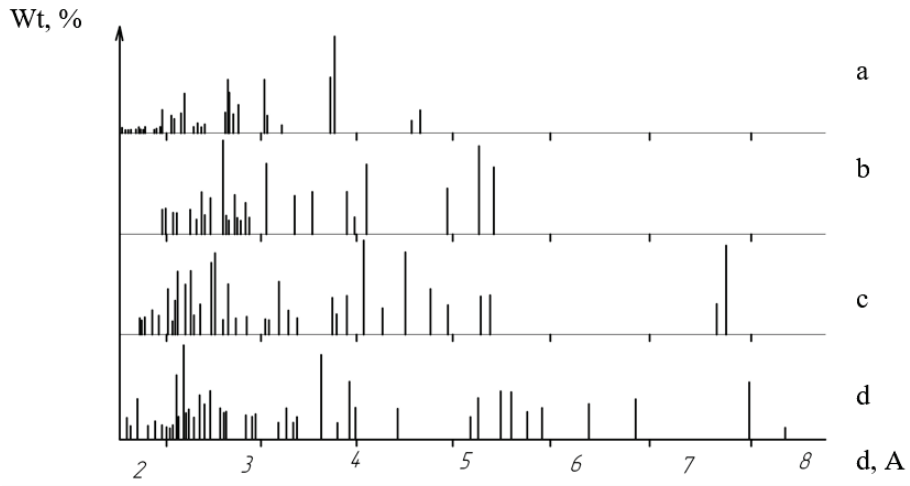

FIGURE 3. *A stroke X-ray chart of initial salts of nitrates: a) potassium, b) neodymium and identified coordination compounds, c) $K_2[Nd(NO_3)_5(H_2O)_2]$; d) $K_3[Nd_2(NO_3)_9] \cdot H_2O$*

The used tools made it possible to investigate physical and chemical transformations in the resulting compounds under the influence of heat and confirmed their identity.

The results of the research

By physical and chemical methods in water-salt system of neodymium nitrates and potassium at 50°C between structural components there were found the exchange interactions with the formation of 2 new anionic coordination compounds. The number, composition, concentration limits of crystallization phases coexisting in the system, the nature of their solubility were studied. The phase diagram of solubility was built. Concentration limits of saturated solutions from which the complex nitrates appear coincide with compositions of nonvariant points of solubility isotherms. All possible types of compounds were found. They are all synthesized in a single crystal form. The systematic study of some of their properties was carried out.

In the studied water-salt systems with the increase of the activation energy of heating the complexometric ability of Ln increases. Competing processes of substitution of H_2O molecules on NO_3^- group in presence of Ln^{3+} create conditions for formation of corresponding high symmetric complexes. The different ways of their spatial packing with other structural elements in the crystallization process leads to separation from a liquid phase of anionic coordination compounds of definite composition and structure. The processes of complex formation are affected by the nature of the central atom-complexformer, directed effect on the solutions structure of available singly charged cations (e.g., K^+), the concentration and character of thermal motion of structural elements. A significant effect of the temperature factors, the need for some activation energy for such transformations and their staging were found. The found peculiarities of the aggregate behavior of structural elements in the studied system indicate that the leaky competing reactions are strong technological factors significantly affecting the changes of the lanthanides structural forms activity.

The authors have also studied thermography of the solid phases formed in the system of neodymium nitrates and potassium to explain some regularities that occur in the studied processes of synthesis of

oxide rare earth-containing functional materials, as well as for comparison characteristics that confirms the identity of the received new coordination compounds. The given information of KNO_3 behavior is based on references data [19-22]; $Nd(NO_3)_3 \cdot 6H_2O$ (Fig. 4), $K_2[Nd(NO_3)_5(H_2O)_2]$, $K_3[Nd_2(NO_3)_9H_2O] \cdot H_2O$ – on data from our own studies (Fig. 5, Tables 2, 3).

Thermal decomposition of $Nd(NO_3)_3 \cdot 6H_2O$ is of a complex character (Fig. 4).

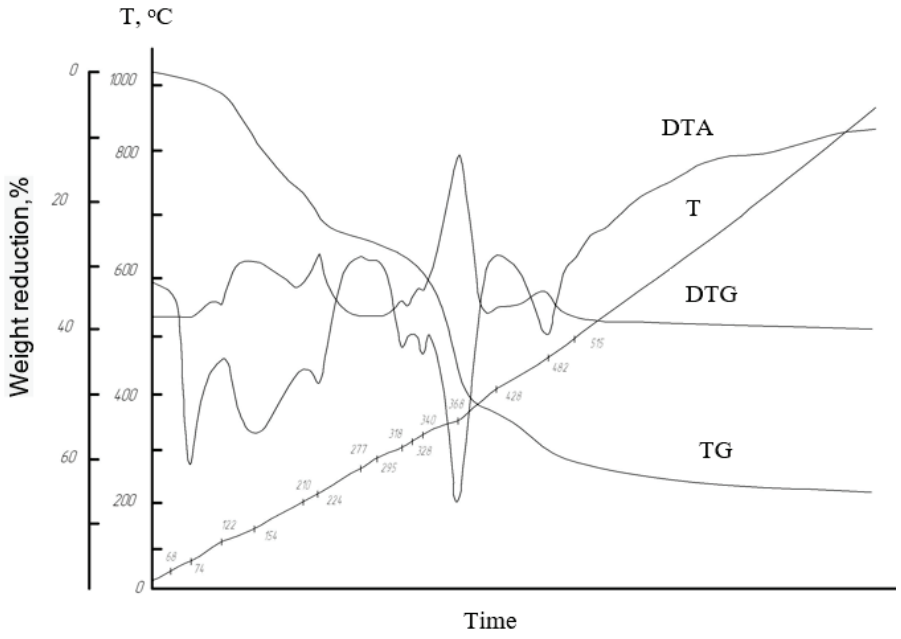

***FIGURE 4**. Derivatograph $Nd(NO_3)_3 \cdot 6H_2O$*

The obtained results are consistent with the data given in a work [23]. At 74°C $Nd(NO_3)_3 \cdot 6H_2O$ it melts in crystallization water (start melting point is 68°C). In temperature range of 74-224°C conversions happen in viscous liquid metastable phase, due to instability of its crystallohydrate forms. The peaks on the curves DTA, DTG with extremes 154°C, 224°C correspond to end effects that overlap and are linked with dehydration of a sample according to the scheme:

$$Nd(NO_3)_3 \cdot 6H_2O \xrightarrow{68\text{-}122^\circ C} Nd(NO_3)_3 \cdot 5.5H_2O \xrightarrow{122\text{-}210^\circ C} Nd(NO_3)_3 \cdot 1.5H_2O \xrightarrow{210\text{-}277^\circ C} Nd(NO_3)_3$$

Anhydrous neodymium nitrate exists in the temperature interval 277-295°C. This is indicated by the dominance of relations Nd-ONO_2 in the melt crystallohydrate forms of neodymium nitrate in spectroscopic studies [24] and clear stoichiometry and composition of complex oxynitrates formed at later stages of decomposition.

The fact of existence of $Nd(NO_3)_3$ simplifies elemental analysis of studied samples and allows to do analytical determinations according to dry residue. In [23] on the base of data from chemical, thermal analyses the scheme of further decomposition of $Nd(NO_3)_3$ is proposed:

$$4Nd(NO_3)_3 \xrightarrow{295\text{-}345^\circ C} Nd_4O(NO_3)_{10} + 2NO_2 + \frac{1}{2}O_2 \qquad (330^\circ C)$$

$$Nd_4O(NO_3)_{10} \xrightarrow{345\text{-}395^\circ C} 4Nd\ ONO_3 + 6NO_2 + 1\frac{1}{2}O_2 \qquad (356^\circ C, 365^\circ C)$$

$$10Nd\ ONO_3 \xrightarrow{395\text{-}500^\circ C} Nd_{10}O_{13}(NO_3)_4 + 6NO_2 + 1\frac{1}{2}O_2 \qquad (450^\circ C)$$

According to our data, Nd_2O_3 is formed above 515°C. Thermal transformations identified in water-salt system of potassium coordination compounds of neodymium (representative of the cerium subgroup) and terby (representative of yttrium subgroup) [25] were studied up to 1000°C and shown in (Fig. 5).

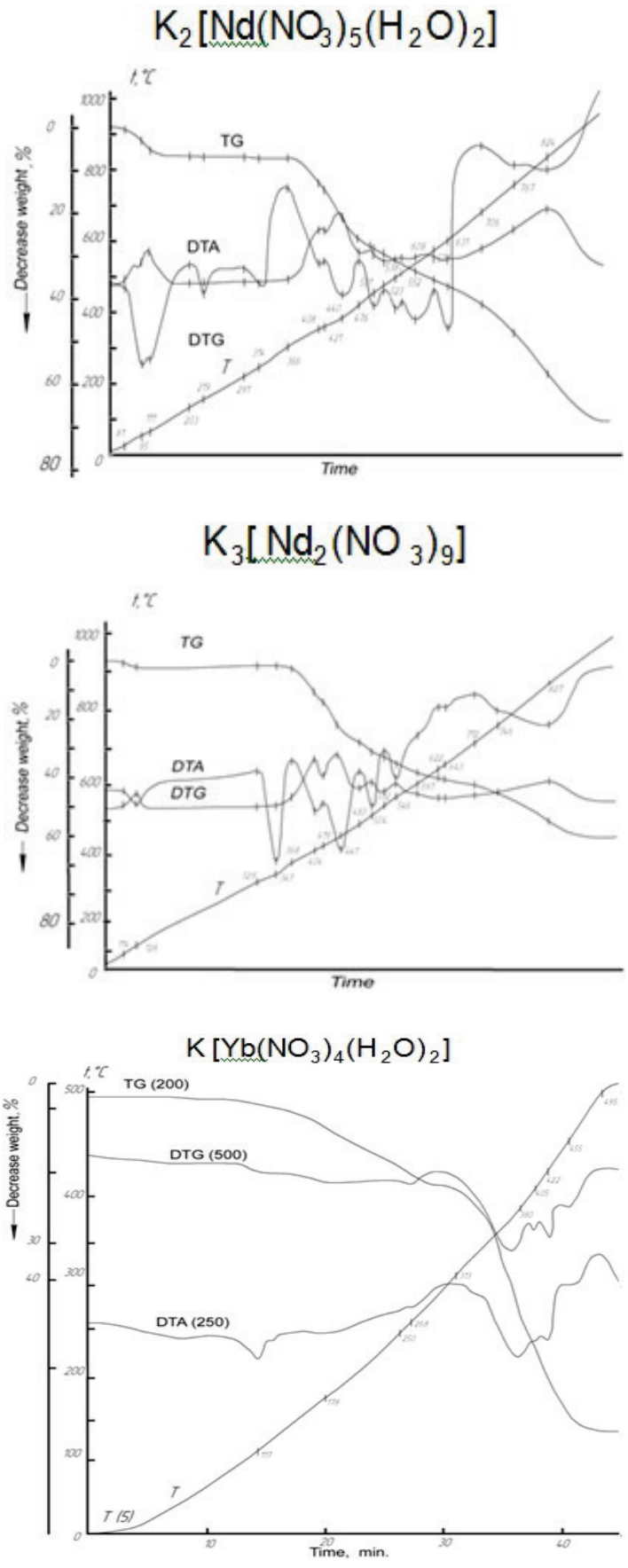

FIGURE 5. *Derivatograph chart of potassium coordination nitrates of neodymium and therby*

The temperature values of the identified effects, their character and nature are systematized and summarized in Tables 2, 3. The obtained data allow the identification of phases. A number of characteristics and laws was found. Their justification from the positions of competing processes is being done.

TABLE 2. *Temperature of representatives transformations of the coordinating group of REE nitrates*

Compounds	Representatives	Dehydration	Melting in crystallization water	Polymmorph transfer	Melting of anhydrous form	Note
$K_2[Ln(NO_3)_5(H_2O)_2]$	La-Nd	95.111	95	219	314	cerium subgroup, values for coord. compounds Nd
$K_3[Ln_2(NO_3)_9]\cdot H_2O$	La-Sm	126	–	–	347	cerium subgroup, values for coord. compounds Nd
$K[Ln(NO_3)_4(H_2O)_2]$	Y, Gd-Lu	138.172	138	–	–	yttrium subgroup, values for coord. compounds Yb

TABLE 3. *The composition of thermolysis products (air, 980°C) of coordination nitrates REE, Y and potassium according to the XRD*

Compounds	Representatives	Composition of transfer products
$K_2[Ln(NO_3)_5(H_2O)_2]$	La-Nd	$KLnO_2$, Ln_2O_3
$K_3[Ln_2(NO_3)_9]\cdot H_2O$	La-Sm	Ln_2O_3
$K[Ln(NO_3)_4(H_2O)_2]$	Y, Gd-Lu	Ln_2O_3

Based on the characteristics of obtaining process of oxide REE-containing functional materials there is an interest to limits of concentration ratios of components to which in phase diagrams the crystallization fields of initial nitrates of rare-earth elements, coordination compounds and their mixtures correspond.

The results of thermal transformations studies of new solid phases found in the model system (see Fig. 5, Tables 2, 3) indicate the different nature of the processes of transformation of compounds of rare-earth elements of cerium and yttrium groups, low and high – temperature of compounds forms of "light lanthanides". Thermograms of elements compounds in the first subgroup are characterized by the formation of anhydrous nitrates. Among compounds with the same name and outer sphere cation the nitrates with a high content of lanthanotus are more heat resistant.

The fact of existence of polymorphism in crystals of composition $K_2[Ln(NO_3)_5(H_2O)_2]$ (Ln-La-Nd) was found. This phenomenon can be explained by the fact that in crystals the disorder occurs due to implementation availability of several distinctive orientations of ions NO_3^-. This kind of disorder is possible due to symmetry of flat NO_3^--ligand, the way of coordinating them by central atom (Ln^{3+} – complexing agents), as well as the method of packing complexes into spatial structure.

The temperature properties of yttrium subgroup compounds are characterized by the absence of stable anhydrous forms of nitrates, low melting temperatures, dehydration from the molten state, the formation of Ln_2O_3 (980°C).

The composition of thermal conversion products (about 980°C) compounds of cerium subgroup depends on the composition of initial nitrates, the degree of volatility of oxides of corresponding alkali metals. In products of thermolysis the compounds $K_2[Ln(NO_3)_5(H_2O)_2]$, except oxides K_2O, contain also their dioxolanthanides $KLnO_2$.

Analysis of the research results with the study of model systems and system analysis of information obtained from scientific publications on the topic of this paper evidents that a positive feature of the use of these REE-containing nitrate systems compared to other soluble systems of chlorides, oxalates is in that, that competing ion exchange interaction leads to easy formation of a whole class of anionic coordination compounds Ln^{3+} with oxygen atoms (electron donors) NO_3^--groups (ligands) of the entire natural range of rare earth elements with all cations of alkali metals, and still stable both in solutions and melts. This allows to carry out technological transformations with a low energy cost (due to low activation energy of the processes of complexation Ln^{3+} with planar small NO_3^--groups). Complex compounds are fusible, little aggressive, elements of cerium subgroup are non-volatile. It allows to work at lower temperatures, the temperature range of stability of complex particles increases.

Conclusions

The results of the study indicate that processes of obtaining REE oxide-containing structural and functional materials for various purposes using nitrates with various elements of electronic structure by chemical mixing the initial components in joint selection of products from the liquid phase by sequential or joint deposition followed by heat treatment happen stage by stage through the formation of several intermediate phases. Their structure, content and behaviour, in each case, require systematic empirical knowledge about their joint behavior in full concentration ratios in a given temperature interval.

The differences in the behavior of structural components in systems lanthanides of cerium and yttrium subgroups, the nature of interaction, stages, characteristics and regularities of flow were found.

New knowledges are the basis for search of ways of increasing the activity of Ln-forms; clarification of the nature of serial thermal transformations of nitrate REE containing multicomponent systems of different aggregate states in the course of their thermal treatment; conditions of formation and existence, properties of intermediate phases; influencing factors; possible methods of control; for creation of modern, perfect low-cost technologies for the synthesis of functional various purposes materials with reproducible properties.

Conflicts of Interest: The author declares no conflict of interest.

References

[1] Mazurenko E.A., *Coordination compounds of metals, precursors of functional materials*/Mazurenko E.A., Gerasimchuk A.I., Trunova E.K. et al., Ukr. Chem. Journe., 2004, Vol. 70, No. 7, pp. 32-37.

[2] Belous A.G., *Complex metal oxides for high-frequency and high-permeability dielectrics*/Belous A.G., Ukr. Chem. Journe., 2008, Vol. 74, No. 1, pp. 3-21.

[3] Melcher C.L., Nucl. Instr. Methods in Phus. Res, 2005, Vol. 1, A 537, pp. 6-14.

[4] Yanagida T., Roh T. et al., Nucl. Instr. Methods in Phus. Res., 2007, Vol. 1, A 579, pp. 23-26.

[5] Gavrilenko O.M., *Crystallochemical features and properties of Li^+,{Na^+, K^+}-substituted lanthanum niobates and defect-perovskite structure*, Gavrilenko O.M., Pashkova O.V., Belous A.G., Ukr. Chem. Journe., 2005, Vol. 71, No. 8, pp. 73-77.

[6] Solopan S.O., *Synthesis and properties of composite structures based on ferroelectric and magnetic phases*, Solopan S.O., Vunov O.I., Kovalenko L.L. et al., Ukr. Chem. Journe., 2006, Vol. 72, No. 1, pp. 28-31.

[7] Kobylianska S.D., *Synthesis of nanoscale systems (Li, La){Ti, Nb}O_3) by Sol-gel method*, Kobylianska S.D., Gavrilenko S.D., Gomza Y.P., Ukr. Chem. Journe, 2010, Vol. 76, No. 4, pp. 84-88.

[8] Durilin D.A., *Synthesis, structure and properties of solid solutions $La_{0,7}Ca_{0,3-x}Na_xMnO_3$*, Durilin A.A., Yanchevskii A.H., Tovstolytkin A.I. et al., Ukr. Chem. Journe., 2004, Vol. 70, No. 9, pp. 34-37.

[9] Gavrilenko O.M., *Li leading materials based on niobates and lanthanum tantalates: synthesis, structure, properties*, Gavrilenko O.M., Ukr. Chem. Journe., 2004, Vol. 70. No. 9, pp. 31-34.

[10] Mittra R., *Critical look at metamaterials*, Radio Engineering and Electronics, 2007, Vol. 52, No. 9, pp. 1051-1058.

[11] Belous A.G., *The influence of the method of obtaining of phase transformations, structure and magnetoresistive properties of manganites $La_{0,7}Sr_{0,3}MnO_{3y}$*, Belous A.G., Pashkova E.V., Vunov O.I. et al., Ukr. Chem. Journe., 2005, Vol. 71, No. 5, pp. 17-23.

[12] Titov Y.O., *Feature means of creation of layer scandates $SrLn_nSc_nO_{3n+1}$ from systems of crystallized nitrates*, Titov Y.O., Slobodyanik M.S., Kraevska Y.A. et al., Ukr. Chem. Journe., 2010, Vol. 76, No. 5, pp. 11-16.

[13] Pashin C.F., Antipov E.V., Kovba L.M., *Influence of cation substitution in solid solutions of YBa_2-x$Sr_xCu_3O_y$ temperature superconductivity*, Superconductivity: physics, chemistry, engineering, 1990, Vol. 3, No. 10, pp. 2386-2389.

[14] Ueda K., 3rd Laser Ceramics Symp, 8-10 October 2007, Paris 2007, pp. IO-C-1.

[15] Kudrenko E.A., Shmitko I.M., Strukova G.K., *Structure of precursors of complex oxides REE obtained by thermolysis of solvent*, Physics of Solid Body, 2008, Vol. 50, No. 5, pp. 924-930.

[16] Smitko I.M., Kudrenko E.A., Strukova G.K., *Initiating continuous action of heating on the phase formation during solid-phase synthesis of complex oxides of rare earth elements*, Letters in GTAF, 2007, Vol. 86, No. 7, pp. 544-548.

[17] Goroshenko Y.G., *Physico-chemical analysis of homogeneous and heterogeneous systems*, Goroshenko Y.G., Naukova Dumka, 1978, p. 490.

[18] Anosov C.Y., *Fundamentals of physico-chemical analysis*, Anosov V.Y., Ozerova M.I., Fialkov Y.Y., M.: Nauka, 1976, p. 503.

[19] Parsonidg N., *Disorder in crystals*, P. 1, Parsonig N., Stably L, M.: Mir, 1982, p. 434.

[20] *Thermal constants of substances*, Vol. 10, Ch. Tables of accepted values, M.: Nauka, 1978, p. 442.

[21] Carling Robert W., *Heat capacities of $NaNO_3$ and KNO_3 from 350 to 800 K*, Thermochim. Acta., 1983, Vol. 60, No. 3, pp. 265-275.

[22] Nissen Donald A., *Thermophysical properties of the equimolar mixture $NaNO_3$ – KNO_3 from 300 to 600°C*, J. Chem. and Eng. Data., 1982, Vol. 27, No. 3, pp. 269-273.

[23] Shurov V.G., Alekseeva O.M., *Thermal graphical studies of decomposition of lanthanide nitrates in range of lanthanum – samarium* [in:] *Thermal analysis and phase equilibria*, Publishing House of Perms, State University, Perm 1982, pp. 38-45.

[24] Turceva T.I., Gliserman V.I., *Spectroscopic study of aqueous solutions of nitrates of rare-earth elements*, Vestnik St. Petersburg University. Mosk. Univ. Chemistry, 1973, Vol. 14, No. 1, pp. 51-54.

[25] Dryuchko A.G., *The use of features of temperature transformations of coordination nitrates REE in production of electronics products*, Dryuchko A.G., Storozhenko D.A., Bunyakina N.V. et al., New Technology, Scientific Herald of KWAITO, 2004, No. 1-2 (4-5), pp. 53-57.

Anastasiya PAVLENKO

Dneprovsky State Technical University, 51900, Kam'yanske, Dniprobudivska, 2, Ukraine

Doi: 10.53412/jntes-2020-4.5

A MATHEMATICAL MODEL BASED ON HEAT CONDUCTION EQUATION FOR PREDICTING AMORPHOUS MASSIVE STRUCTURES

Abstract: *The article presents the results of a study of the process of cooling a liquid molten metal on the surface of rotating rolls. A mathematical model is proposed to determine the optimal ratio of the cooling water temperature and the size of the cooling surfaces. The research results can be used to optimize technological processes associated with the production of thin metal sheets.*

Keywords*: cooling of melts, phase transformations, melt temperature.*

Introduction

Practical problem of determining the dynamics of solidification of the melt in time and prediction metal structure includes the calculation and analysis of temperature fields, determine the velocity of the solidification front in time, can be solved by means of mathematical modeling. For solving this problem mathematical model was developed in the basis, which was supposed to thermal conductivity equation. Formation a continuous layer of metal is complex irreversible process, consisting of a series of simple phenomena, which in this case cannot be considered without interacting with each other. Irreversibility of the process is associated primarily with the irreversibility of heat and mass transfer, the internal motion in the solid and liquid phases. In the general case a quantitative description of the process is based on the consideration of non-equilibrium thermodynamics uninsulated heterogeneous system consisting of few components, and the phases separated and the environment bounding hull.

Continuous process of pulling the metal layer can be represented as flows of viscous incompressible layer between two elastic-plastic surfaces (rollers), moving with a certain velocity (Fig. 1). Moreover, for an arbitrarily selected point in the cooling layer is characterized by a continuous change in temperature, pressure (stress), speed, distance to the boundary of the transition from liquid to solid state.

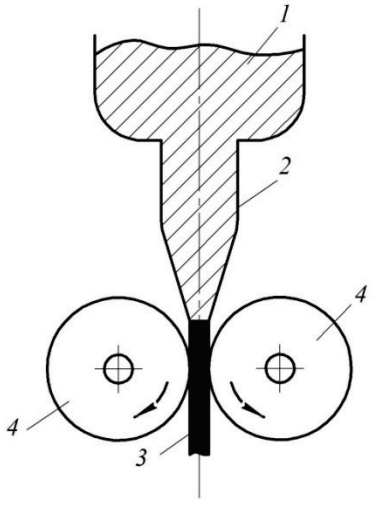

Figure 1. *Scheme of pulling process of a continuous layer of metal: 1 – the liquid metal melt; 2 – form for the metal; 3 – cooled metal layer; 4 – cooled rollers*

Thus, consideration of the cast layer (3) is bounded on both sides by curved surfaces (rollers) (4). Layer (3) is viscous incompressible fluid.

Formalization of the mathematical model

Since the problem of the motion of continuously cast layer is closely related to the problem of heat exchange, the key is to thermal conductivity equation in a general form for a moving continuous medium (layer 3) in which there are distributed sources of heat of the phase transition, depending on the specific heat of phase transition [1]:

$$\rho \cdot \frac{\partial}{\partial t}\left[c(T)T - L\Psi\right] = \mathrm{div}\left[\lambda(T)\mathrm{grad}T\right] + Q_v \tag{1}$$

and Fourier law thermal conductivity $q = -\lambda(T)\mathrm{grad}T$;

where:

ρ – density;

c – thermal capacity;

λ – thermal conductivity;

T – temperature;

L – specific heat of the phase transition (solidification);

Ψ – the proportion of solid phase (the liquid phase $\Psi = 0$, for the solid phase $\Psi = 1$, in the mushy zone $0 < \Psi < 1$);

$Q_v(x, y, z, t)$ – function characterizing the amount allocated during the solidification heat.

To obtain a unique solution of the problem is necessary to supplement its initial and boundary conditions [2, 3]:

$$\lambda_m \frac{\partial T}{\partial x} = 0 \tag{2}$$

$$x = \frac{H}{2} \;\; \lambda_m \frac{\partial T}{\partial x} = \alpha\left(T_m - T_a\right) \tag{3}$$

where:

T_m – metal temperature, °C;

T_a – air temperature, °C.

$$T(x,0) = 1300\,^{\circ}\mathrm{C} \tag{4}$$

At the phase boundary solid metal – liquid melt is given by the boundary condition of Stephen:

$$\lambda_1 \frac{\partial T_1(t,\xi(t))}{\partial n} - \lambda_2 \frac{\partial T_2(t,\xi(t))}{\partial n} = L\frac{d\xi(t)}{dt} \tag{5}$$

where:

$\xi(t)$ – equation of the curve separating phases solid metal – liquid melt;

L – heat change of state, J/K (empirically determined value for the transition of the liquid melt in the solid metal);

n – normal to the curve;

$T_1(t,r)$ – temperature of the solid phase (solid metal);

$T_2(t,r)$ – temperature of liquid phase (liquid melt);

λ_1 – temperature diffusivity coefficient of the solid metal;

λ_2 – temperature diffusivity coefficient of the liquid melt.

Define the shape of the curve $\xi(t)$. We seek a solution of the thermal conductivity equation (1) in the following automodel form:

$$T(t,r)=f(z), \quad \text{where} \quad z=\frac{r}{\sqrt{t}} \tag{6}$$

Substituting (6) into (1) leads to the following ordinary differential equation:

$$-\frac{1}{2}f'(z)\cdot z=\lambda\left(f''(z)+\frac{1}{z}f'(z)\right) \tag{7}$$

From which:

$$f(z)=C_1\int\frac{\exp\left(-\frac{z^2}{4\lambda}\right)}{z}dz+C_2 \tag{8}$$

where C_1 and C_2 are arbitrary constants of integration.

Next to finding the shape of the curve $\xi(t)$, we substitute (6) into the boundary condition Stephen (5). We get:

$$\lambda_1\frac{1}{\sqrt{t}}f_1'\left(\frac{\xi(t)}{\sqrt{t}}\right)-\lambda_2\frac{1}{\sqrt{t}}f_2'\left(\frac{\xi(t)}{\sqrt{t}}\right)=L\frac{d\xi}{dt}$$

from which:

$$\frac{\xi(t)}{\sqrt{t}}=\alpha=\text{const}$$

$$\lambda_1 f_1'(\alpha)-\lambda_2 f_2'(\alpha)=\frac{L}{2}\alpha \tag{9}$$

Consequently:

$$\xi(t)=\alpha\sqrt{t} \tag{10}$$

where the coefficient α is defined as the solution of the transcendental equation (9) with the known value of L aggregate heat transition molten liquid to the solid state.

Knowing the equation of the curve $\xi(t)$, separating the liquid melt phase – solid metal, we can reduce solution of original problem to the solution of the thermal conductivity equation with generalized (discontinuous) temperature conductivity coefficient:

$$\frac{\partial T}{\partial t}=\lambda(t,r)\left(\frac{\partial^2 T}{\partial r^2}+\frac{1}{r}\frac{\partial T}{\partial r}\right)$$

where:

$$\lambda(t,r)=\begin{cases}\lambda_1, \text{if } 0\le r<\theta R+\xi(t)\\ \lambda_2, \text{if } \theta R+\xi(t)\le r<R\end{cases}$$

Initial conditions:

$$T\big|_{t=0}=T_m \quad at \quad 0\le r<\theta R+\xi(t);$$
$$T\big|_{t=0}=T_a \quad at \quad \theta R+\xi(t)\le r<R$$

In Figures 2-4 shows graphs characterizing the dependence of the degree amorphization of the parameters of the pulling process (rapid casting) a metal layer between the cooling rolls.

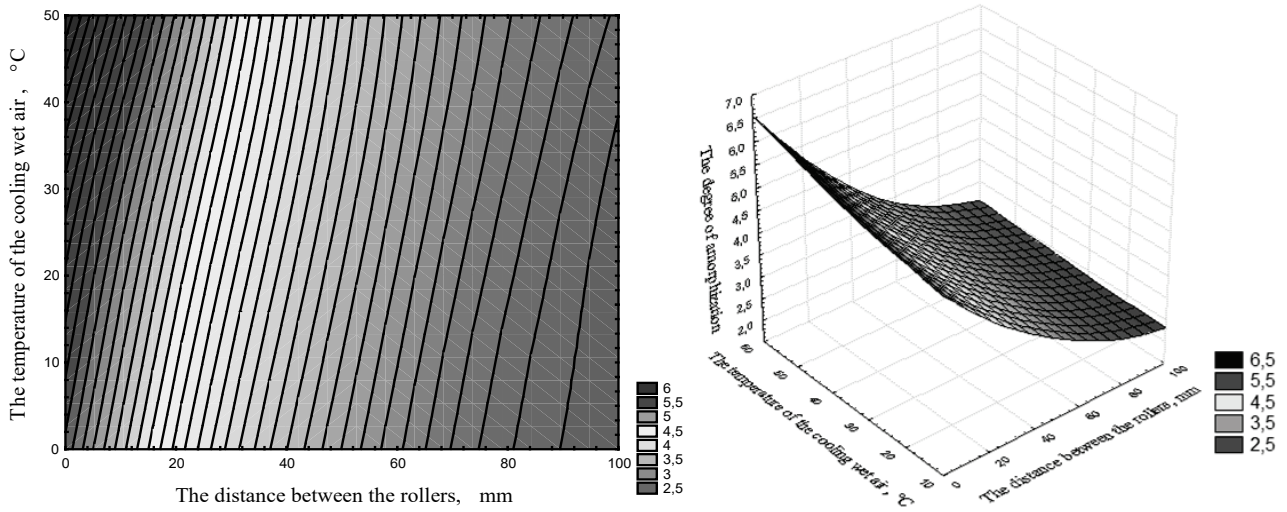

FIGURE 2. *Graph of the dependence of the degree of amorphization from the temperature of the cooling wet air and the distance between the rollers*

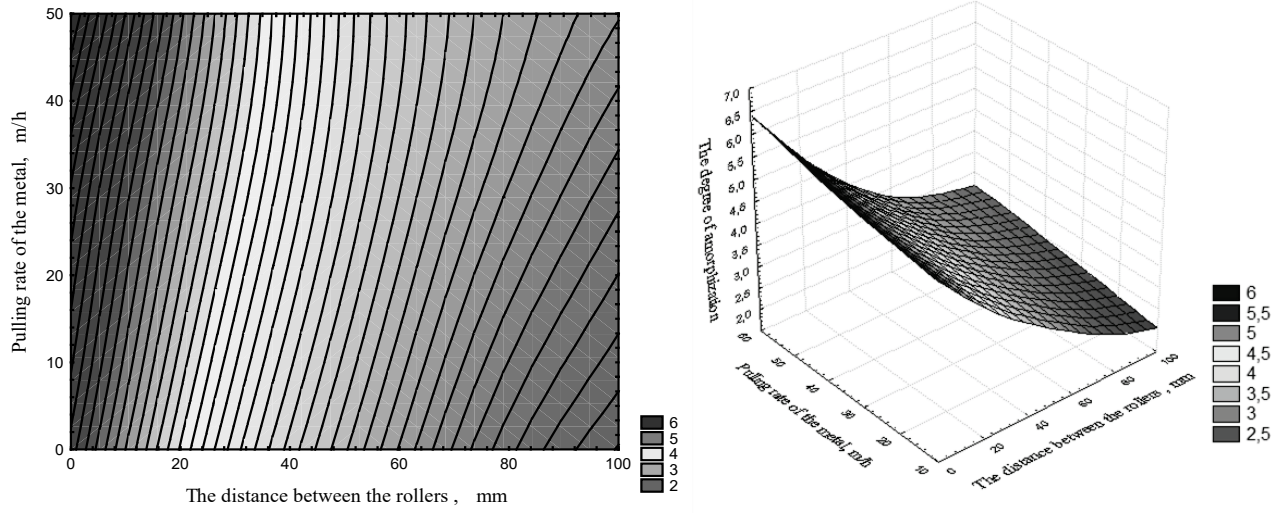

FIGURE 3. *Graph of the dependence of the degree of amorphization from pulling rate of the metal and the distance between the rollers*

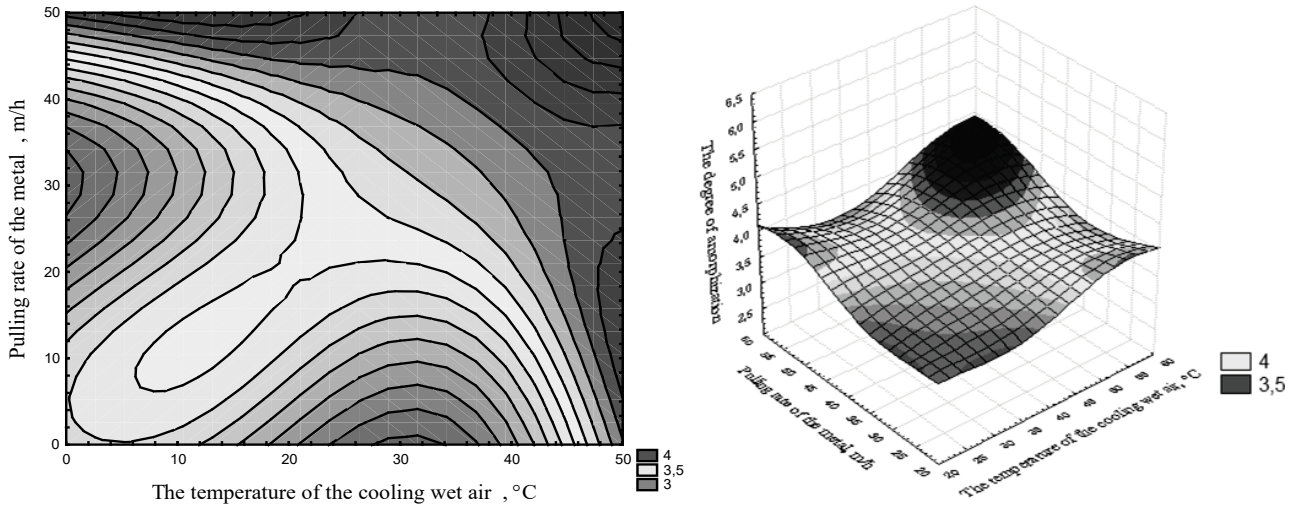

FIGURE 4. *Graph of the dependence of the degree of amorphization from pulling rate of the metal and the temperature of the cooling wet air*

Conclusions

1. Practically proved that under certain modes of the pulling process (rapid casting) metal layer between the cooling rolls is possible to obtain an amorphous structure at the layer boundaries.
2. To obtain an amorphous structure of the metal process pulling (fast casting) implement only when such interaction mode parameters (control factors) as the distance between the rollers, pulling speed of the metal and the temperature of the cooling wet air. To increase the degree of amorphization of the casting process is necessary to increase the temperature of the cooling wet air and pulling speed of the melt. But the main parameter of the process that has the greatest impact on the degree of amorphization of metal is the distance between the rollers. At the minimum values of distance degree of amorphization has a maximum value.

Conflicts of Interest: The author declares no conflict of interest.

References

[1] Pavlenko A.M., Usenko B.O., Koshlak H.V., *Analysis of thermal peculiarities of alloying with special properties*, Metallurgical and Mining Industry, 2014, No. 2, pp. 15-19.

[2] Pavlenko A.M., Usenko B.O., Koshlak H.V., *Analysis of thermal processes in the surface layer formation with amorphous structure*, Metallurgical Processes and Equipment, 2014, 2(36), pp. 15-19.

[3] Pavlenko A.M., Usenko B.O., Koshlak A.V., *The thermophysical aspects of structure formation of amorphous metals*, Transactions of Academenergo, 2014, No. 1, pp. 7-16.